



Availability of the current and future water resources in Central Africa, case of the large Sanaga catchment in Cameroon

Valentin Brice Ebodé^{a,b,*}, Jean Guy Dzana^b, Raphael Onguéné^c, Sakaros Bogning Dongué^c, Bérenger Koffi^d, Jean Riotte^e, Gil Mahé^f, Jean Jacques Braun^a

^a International Joint Laboratory DYCOFAC, IRGM-UY1-IRD, BP 1857, Yaounde, Cameroon

^b Department of Geography, University of Yaounde 1, P.O. Box 755, Yaounde, Cameroon

^c University Institute of Technology, University of Douala, Douala, Cameroon

^d Laboratory of Science and Technology of Environment, Jean Lorougnon Guédé University, BP 150, Daloa, Côte d'Ivoire

^e Indo-French Cell for Water Sciences, Joint IRD-IISc Laboratory, Indian Institute of Science, Bengaluru, India

^f HSM, Univ Montpellier, CNRS, IRD, IMT Mines Alès, Montpellier, France

ARTICLE INFO

Keywords:

Central Africa
Sanaga River basin
SWAT
Regional climate models
Climate variability
Land use and land cover changes

ABSTRACT

Study region: Mbakaou and Bamendjing basins (Sanaga River sub-basins).

Study focus: In this study, the availability of water resources was assessed over the period 2002–2019, based on the SWAT (Soil and Water Assessment Tool) hydrological model and certain meteorological and spatial reference data available for the region (Merra2, Landsat, etc.). Forecasts of its evolution were then made with the same tool (SWAT) over two futures periods (near 2024–2035 and medium: 2036–205) based on data from four (04) regional climate models (RCMs) (CCCma, HIRHAM5, RCA4 and REMO) and future land use and land cover (LULC) data simulated using the CA-Markov procedure. To separate the impact of climate variability (CV) and land use and use and land cover changes (LULCCs) on future water resources, two evolution scenarios (experiments) were established: (1) the impact of the CV, by associating future climate data with LULC from the historical period; (2) the impact of LULCCs, by combining future LULC maps with climate data from the historical period.

New hydrological insights for the region: The performances of the SWAT model are satisfactory in calibration and validation on the two basins with R^2 , NSE and KGE greater than 0.68. Two models (CCCma and REMO) predict a decline in water resources in these basins, and two others (HIRHAM5 and RCA4) the opposite. The REMO model seems the most reliable. It predicts a drop in precipitation and runoff (SURQ) in the two basins that do not respectively exceed –19% and –31%. CV is the only forcing whose impact will be visible in the dynamics of future water resources, given the insignificant changes expected in the evolution of LULC patterns. The results of this study could contribute to improving the management of water resources in the studied basins and the region.

* Corresponding author at: International Joint Laboratory DYCOFAC, IRGM-UY1-IRD, BP 1857, Yaounde, Cameroon.

E-mail address: ebodebriso@gmail.com (V.B. Ebodé).

¹ <https://orcid.org/0000-0003-3307-4789>

<https://doi.org/10.1016/j.ejrh.2024.101815>

Received 12 September 2023; Received in revised form 1 May 2024; Accepted 5 May 2024

Available online 14 May 2024

2214-5818/© 2024 The Authors. Published by Elsevier B.V. This is an open access article under the CC BY license (<http://creativecommons.org/licenses/by/4.0/>).

1. Introduction

The efficient management of water resources is an arduous task that requires good knowledge of the quantity of existing resources, good understanding of processes underway and reliable hydroclimatic forecasts (Lambin et al., 2003; Ebodé, 2023). However, the sub-Saharan African countries, in general, and those of Central Africa, in particular, do not have good quality information concerning the availability of this resource, including in basins of particular interest (those hosting dams, for example), and for good reason, the lack of observed data. The active network in this part of the continent now only includes 35 stations for the Democratic Republic of Congo (i.e. 1 station for 67,000 km²), 22 stations for Cameroon and less than 20 stations for Gabon, Congo and the Central African Republic as a whole (Bigot et al., 2016). This lack of data prevents any attempt that could help to understand the issue of water resource availability and its future evolution, in particular the hydrological modelling that is widespread elsewhere. Despite its limitations, hydrological modelling represents one of the best alternatives to quantify the availability of this resource and predict its evolution for better management (Dosdogru et al., 2020).

Hydrological modelling is approached differently in the literature, although several approaches may be combined in a single study (Hyandy et al., 2018; Dibaba et al., 2020). Some authors focus on understanding watersheds and quantifying available water resources (Yin et al., 2017). Using the SWAT model, Faramarzi et al. (2009) quantified the availability of water resources in Iran. The results obtained in calibration and validation are satisfactory. The averages of the main water balance components (WBCs) were quantified by sub-basins. According to them, irrigated agriculture has a high impact on these WBCs. The resulting vulnerability of water resource availability has implications for the country's food security. Similarly, the hydrological water balance analysis of the Lake Tana basin in Ethiopia indicated that baseflow is an important component of the total discharge within the study area that contributes more than the surface runoff (Setegn et al., 2010).

Other authors seek to understand the factors influencing the availability and variability of this resource (Ebodé et al., 2022). In a study conducted in the Zhangweinan basin, Ziyang Zhao et al. (2020) demonstrated that the human factor (urbanization) has the greatest influence on the variability of water resources. They showed that the decrease in runoff caused by this factor is four times greater than that caused by the natural factor (climate variability/change). Zhang et al. (2020) have shown in the context of the Ganjiang basin (China) that it is climate change that has the greatest influence on the water balance components (WBCs) variability. This forcing is correlated positively with runoff and discharge. In the same vein, Elaji and Ji (2020) demonstrated in their study on the Kansas basin that urbanization did not influence the observed and simulated flow during the two years studied (2003 and 2017). Devising ecologically sound watershed management and development plans, and gaining insights into the implications of the present land-use management practices were achieved through applying the SWAT model to evaluate the impact of agricultural conservation practices on water and sediment yield (Mwangi et al., 2015). It appears that land-management practices such as using filter strips can reduce the annual evapotranspiration and increase streamflow, as assessed using the SWAT model. Such land-management practices could have great potential to mitigate the impacts of land use/cover changes on water resources, thus increasing water resource availability.

There is also another category of authors who seek to predict the availability of water resources (Ardoin et al., 2009; Chang and Jung, 2010; Ruelland et al., 2012; Mendez and Calvo-Valverde, 2016; Hadour et al., 2020). Yira et al. (2017) attempted to predict the variability of flows from the outputs of regional climate models (RCMs). Their results revealed that future simulated flows have many uncertainties. For them, these results are difficult to exploit insofar as some outputs predict an increase and some others a decrease. Thus, adaptation strategies to future hydroclimatic changes should take into account these two hypotheses. Awotwi et al. (2021) highlighted in their study on the Pra basin in Ghana an increase in flows for the middle of the 21st century and a decrease for the end. These trends concern the RCP4.5 emission scenario. For the RCP8.5 scenario, they projected an increase throughout the century. In their study on the Ndembera basin (Tanzania), Hanye et al. (2018) postulated that during the period from 2013 to 2020, the agricultural land and evergreen forests will increase by nearly 10 and 7%, respectively. Mixed forests will decrease by 12%. Such land use/cover changes will decrease the total water yield by nearly 13% while increasing evapotranspiration and surface runoff by approximately 8 and 18%, respectively. This moisture balance changes will be aggravated by warmer near-future mean annual temperatures (1.1 °C) and wetter conditions (3.4 mm/year) than in the baseline period (1980–2009). The warmer future climate will increase evapotranspiration and decrease water yield by approximately 35 and 8%, respectively. Zhang et al. (2019) projected for the Manning basin (Australia) a decrease in precipitation and runoff over the period 2021–2060, and an increase over the period 2061–2100. According to them, evapotranspiration is expected to experience a slight increase and the reverse is expected for soil water capacity.

Modelling work aiming at predicting the availability of water resources is partly based on RCMs data (Reshmidevi et al., 2018). Although it is one among the main means available to the scientific community so far for such investigations, it should be emphasized that the reliability of these data is problematic (Chen et al., 2012). Facing this situation, some authors suggest combining several RCMs to reduce uncertainties (Knutti et al., 2010; Zhang and Huang, 2013). It is this approach that is adopted in this study. However, we will try to go further by proposing, after a statistical analysis over the historical period, the model whose forecasts seem the most reliable.

Predictive hydrological modelling can be done using a global or distributed/semi-distributed approach. In the global approach, the watershed is considered as a single entity. GR2J (rural engineering model with two daily parameters) and GR4J (rural engineering model with four daily parameters) are some of the reference models generally used in this approach (Bodian et al., 2012). The parameters mainly taken into account in the latter are precipitation, evapotranspiration and, to a lesser extent, soil water capacity. On the other hand, in the distributed/semi-distributed approach, the watershed is considered as a more complex entity. Flow modelling here requires a subdivision into homogeneous elementary surfaces (Taleb et al., 2019). A wide range of input data (meteorological and spatial) is required. In terms of performance, the distributed/semi-distributed approach has a slight advantage in complex basins as

their physical heterogeneity is considered (Tegegne et al., 2017). This explains our decision to use this approach to study a forest-savanna transition zone where the global approach could not produce satisfactory results (Sighomnou, 2004). Several distributed/semi-distributed hydrological models have been developed to simulate the hydrological processes of watersheds and predict flows (Beven and Kirkby, 1979; Abbott et al., 1986; Arnold et al., 1998). Because most of them only allow an approximate characterization of the physical environment of the watershed using data and parameters in a point-grid network (Wang et al., 2012), SWAT appears to be one of the top hydrological models capable of adequately simulating flows in complex environments in the wide range of existing models (Akoko et al., 2021), reason why it has been chosen in this study.

The Sanaga watershed is the largest entirely included in Cameroonian territory. It is also the one with the most significant quantity of water resources, which could explain why it is currently full of four (04) reservoir dams (Mbakaou, Bamendjing, Mape and Lom Pangar) and that others are under construction (Nachtigal dam). This could also explain the drinking water supply to the Yaounde city (political capital of Cameroon) from this basin. Climate change and poor management of available water resources are often the reasons justifying the frequent power cuts observed in the regions supplied by the hydro-electricity produced from this basin. The management of this water resource could be based on the modelling of the entire basin. However, given the complexity of such an operation on the scale of such a large (130,055 km²) and complex basin (between two different ecological zones: forest in the South and savannah in the North), it would be good to do so step by step. Proceeding step by step will allow us to know what are the reliable alternative data on which we could rely for such work in such a poorly measured context. This will also provide an idea of how the sub-basins of each ecological zone over which the basin extends operate. All this information will ultimately make it possible to create a reliable model for this basin. It should also be noted that some attempts to model the entire basin have been made, but they failed due to models used (GR2M: rural engineering model with two monthly parameters) and the scarcity of meteorological data (Sighomnou, 2004). This stage of work can be done in several ways, but we have chosen to begin it with the regulated sub-basins modelling, from the oldest to the most recent, because they already have an interest, and the results of this study could be used for their management. The Mbakaou and Bamendjing sub-basins meet these criteria, so this stage of work will begin with them.

Even though they each house a reservoir dam, the Mbakaou and Bamendjing basins have never been the subject of modelling work with the data, approaches and tools mentioned above. Also, forecasts of future water resource availability have never been made. Yet such studies could produce information to improve the management of this resource and the production of hydroelectricity. On the world plan, the impact of climate variability (CV) and land use and land cover changes (LULCCs) on runoff has never been separated in the relevant existing studies using score calculation, as we did in this study. Most studies dealing with these points are often limited to the dominant forcing indication in the behaviour of a given water balance component (WBC). For example, an increase in runoff, while precipitation decreases, is a consequence of changes in land use and land cover (LULC) patterns marked by impervious spaces (buildings, roads, bare soil, etc.) increasing to the detriment of the forest (Ebodé et al., 2022). Likewise, a reduction in runoff while the LULC patterns remain practically the same is a drop in rainfall consequence (Dibaba et al., 2018). However, from the scores, we can easily deduce the impact rate of each forcing on a given WBC, allowing us to make much more appropriate management choices. Finally, even considering the word as a whole, almost no study devoted to hydrological forecasts has ever identified the most reliable climate model. Most studies often consider the average of all models as the most reliable forecast. Yet, excessive bias in a model could impact the average of all models and the forecast distortion. The best is to identify the most reliable models, as we did in this study.

This paper has as objectives to (1) evaluate the capacity of the SWAT model to simulate flows in a watershed with a complex

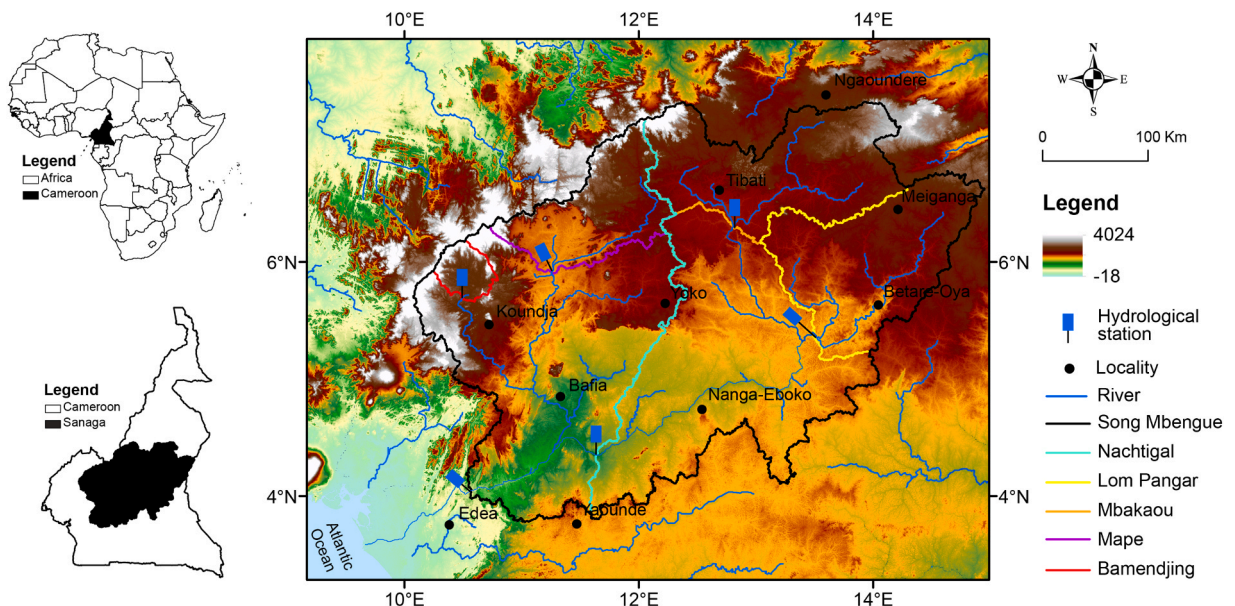


Fig. 1. Location of the Sanaga basin and studied subbasins (Mbakaou and Bamendjing). Source: Ebodé (2022).

physical environment but very little gauges (2) use the model to simulate future flows (near 2024–2050 and average: 2036–2050) in the basin under different climate change scenarios (RCP4.5 and RCP8.5) (3) identify the most reliable climate forecast model in the basin and (4) separate the respective impact of the LULCCs and the CV on the evolution of future water resources. The biggest challenge to hydrological modelling with the SWAT model in the absence of sufficient flow and meteorological gauging stations in basins is to find datasets that can allow to achieve good results like those obtained in this work. The ability of the SWAT model to simulate flows in this poorly gauged basin will be of great importance for socioeconomic development considering the number of construction projects (dams and bridges) ongoing in the basin.

2. Materials and methods

2.1. Study area

The study focuses on two sub-basins of the Sanaga basin (Fig. 1). These are the Mbakaou (19,757 km²) and Bamendjing (2222 km²) sub-basins. The first extends between longitudes 11°9'E-14°4'E and latitudes 6°2'N-7°4'N. The second extends between longitudes 10°2'E-10°8'E and latitudes 5°65'N-6°1'N. Their discharge is regulated by reservoir dams built in 1969 (Mbakaou) and 1974 (Bamendjing). In addition to electricity production, water is mainly used in this basin for domestic uses and irrigation. The prevailing climate is tropical humid, with annual rainfall ranging between 1400 mm and 1600 mm, which falls mainly during a single rainy season from March to November. The annual average temperatures of these basins vary between 22°C and 27°C. The relief encountered in these basins is rugged, with minimum and maximum altitudes around 1000 m and 2000 m (Figs. 3D and 4D). Vegetation type is dominated by savannah (Figs. 3B and 4B).

2.2. Data and methods

2.2.1. Data sources

2.2.1.1. Spatial data. The spatial data required for this study are of three types; digital elevation model (DEM), land use and land cover map and soil map (Figs. 3 and 4).

The DEM (SRTM: shuttle radar topography mission) data used in this study has a spatial resolution of 30 m (Table 1). It was obtained from the United States Geological Survey website (<https://earthexplorer.usgs.gov/>). DEM was used for delineating

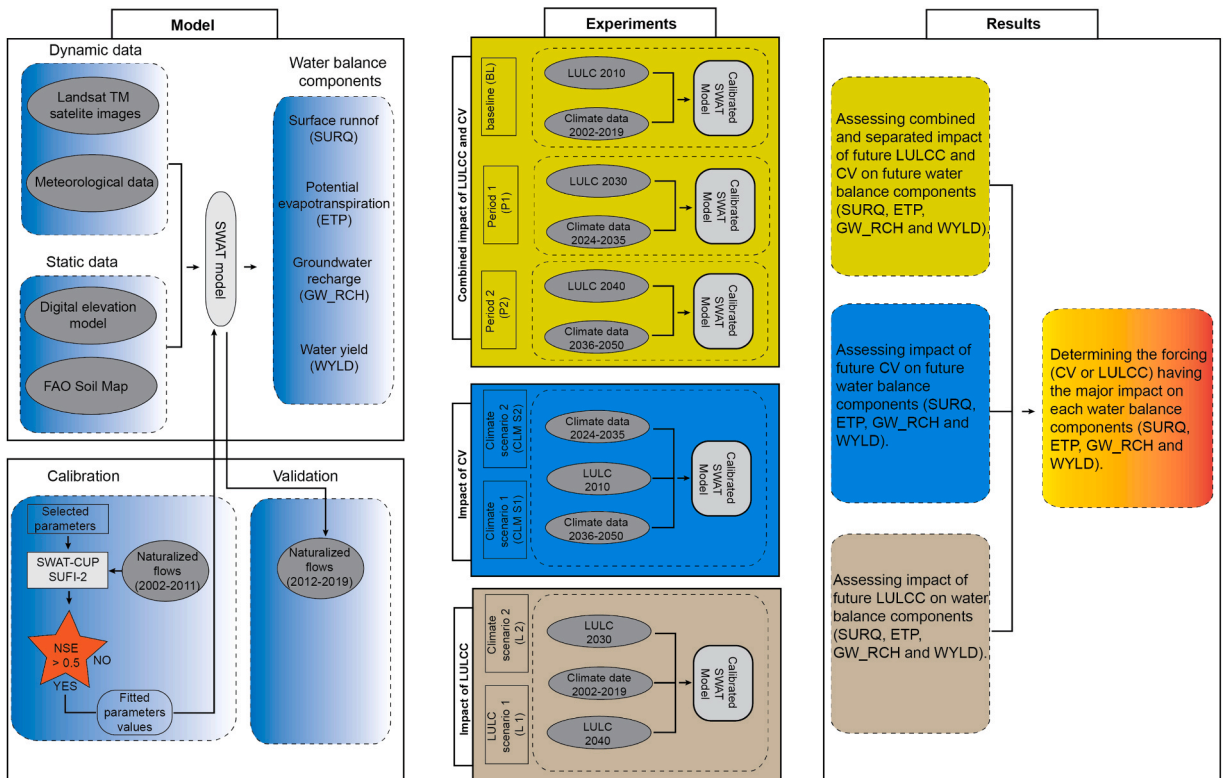


Fig. 2. Study workflow. CLM: climate; L: land use and P: period.

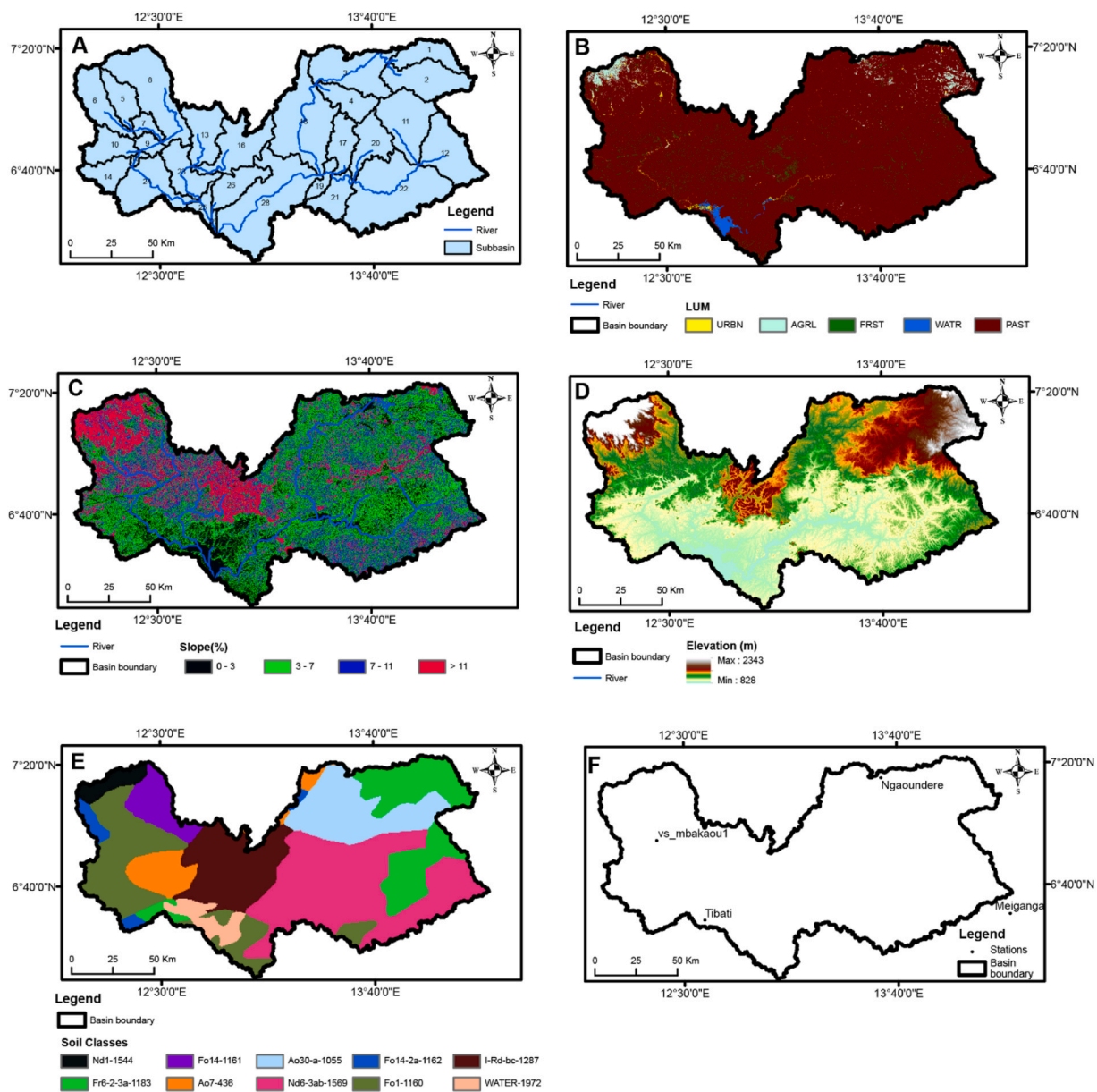


Fig. 3. Spatial data of Mbakaou basin (subbasin boundaries (A), altitudes (D), slopes (C), soils (E) and land use modes (B) and spatial distribution of stations (existing and virtual) (F) used on the SWAT for different simulations.

watersheds, slope classification and generating the hydrological response units (HRUs). In total, 29 and 31 hydrological response units (HRUs) were respectively delineated in the Mbakaou and Bamendjing basins (Figs. 3 and 4).

The food and agriculture organization (FAO) world digital soil map downloaded from the site: <https://storage.googleapis.com/food-catalog-data/uuid/446ed430-8383-11db-b9b2-000d939bc5d8/resources/DSMW.zip> was used as soil data in this study. The soil classification is based on the FAO classification system and was customized as required by the SWAT model (Figs. 3 and 4).

Apart from topographic and soil information, the simulation of flows from the SWAT model requires other information (LULC). Three Landsat satellite images were used to produce historical and predictive LULC maps (Table 1). These are the Landsat 5 image of 1984, Landsat 7 image of 2010, and Landsat 8 image of 2015. The map produced from the image of 2010 was used in the model to simulate the flows during the historical period (2002–2019). The latter presents five (05) main land use and land cover modes (building and road: UBRN; agricultural area: AGRL; forest: FRSE; water body: WATR and bare soils/savannah: PAST) (Figs. 3 and 4). The maps produced from images of 1984 and 2010 were used to predict future LULC for 2030 and 2040. The one produced from the image of 2015 helped to verify the reliability of simulated LULC maps from the method and tool retained.

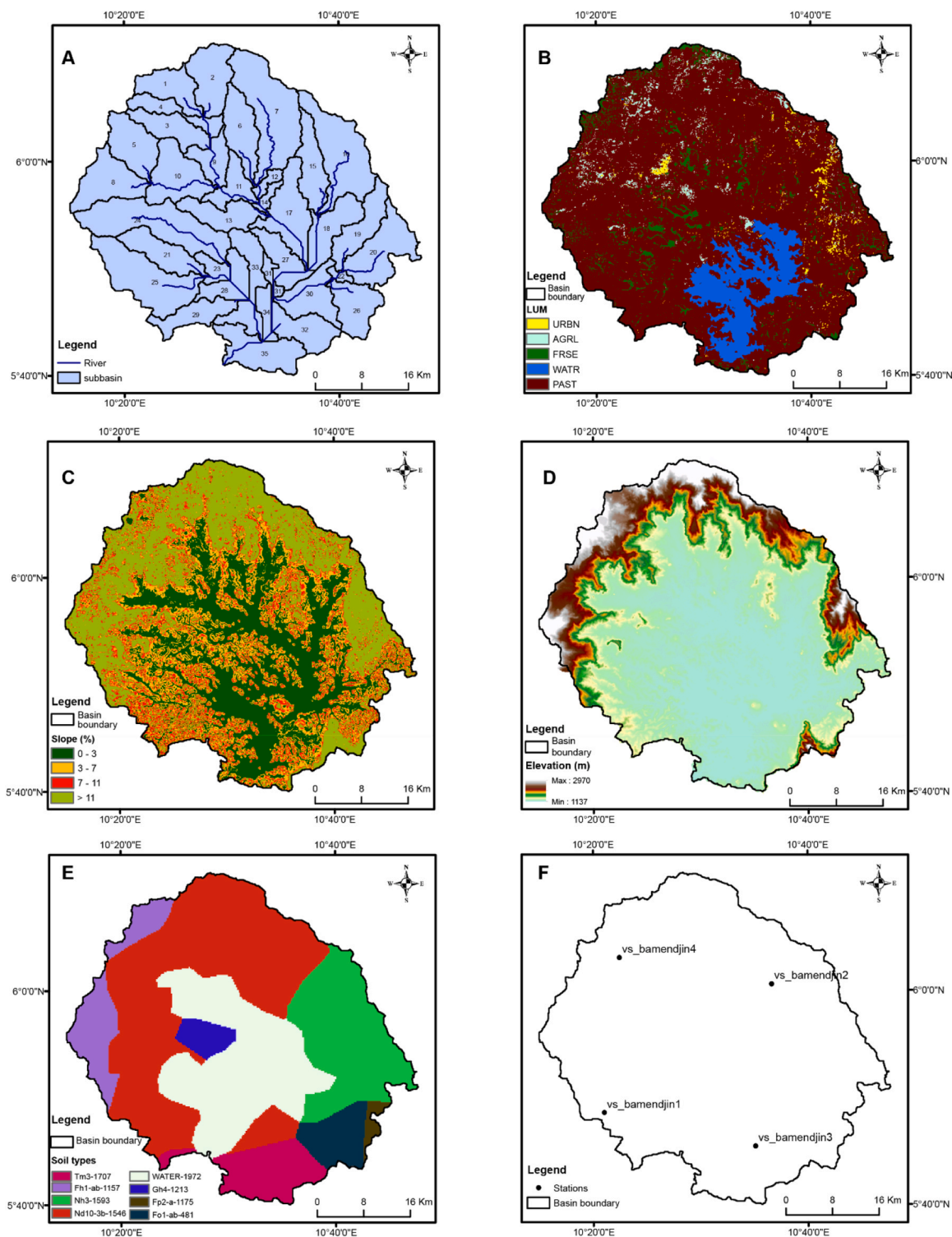


Fig. 4. Spatial data of Bamendjing basin (subbasin boundaries (A), altitudes (D), slopes (C), soils (E) and land use modes (B)) and spatial distribution of stations (virtual) (F) used on the SWAT for different simulations.

2.2.1.2. *Hydrometeorological data.* The meteorological variables needed for runoff modelling with SWAT at daily time step are: maximum and minimum temperatures ($^{\circ}\text{C}$), precipitation (mm/day), relative humidity (%), average wind speed (m/s) and solar radiation (in W/m^2). Rainfall data used are those of the global precipitation climatology project (GPCP). For other parameters, modern-

Table 1
Data used in the study and their characteristics.

Data	Data availability	Spatial resolution	Sources	Purpose of the data use
Shuttle Radar Topography Mission (SRTM)	-	30 m	www.earthexplorer.usgs.gov	Delineating watersheds, slope classification and generating the hydrological response units (HRU)
FAO Digital Soil Map of the World (DSMW), version 3.6	-	1 km	https://storage.googleapis.com/fao-maps-catalog-data/uuid/446ed430-8383-11db-b9b2-000d939bc5d8/resources/DSMW.zip	Extraction of soil data
Landsat 5 satellite image	1984–2013	30 m	www.earthexplorer.usgs.gov/	Creation of land use and land cover maps
Landsat 7 satellite image	1999–2022	30 m		
Landsat 8 satellite image	2013–	30 m	https://giovanni.gsfc.nasa.gov/	Model forcing for flow simulation
Precipitation GPCP (Global Precipitation Climatology Project), version 3.1	2000–2019	0.5°		
Merra2 data (minimum temperature, maximum temperature, wind speed, relative humidity and solar radiation)	1981–2022	0.5°	https://power.larc.nasa.gov/	Model forcing for flow simulation
Regional Climate model (RCM) data from CORDEX project (Rainfall, minimum temperature and maximum temperature).	1950–2100	50 km	https://esgf-data.dkrz.de/search/esgf-dkrz/	Model forcing for flow simulation

era retrospective analysis for research and applications, version 2 (MERRA-2) data were retained. These data were collected in ASCII format at existing and virtual stations (Figs. 3F and 4F). The virtual stations were created for collecting data in all corners of the basins, considering that the model chosen divides the basin into sub-basins and that the meteorological data considered for a given sub-basin are those of the stations closer. GPCP and MERRA-2 represent the most recent data close to observations. They, therefore, constitute a good alternative for modelling flows in ungauged regions.

The flow series used in this study come from the southern interconnected network Cameroon database. These are naturalized flows developed jointly by electricity of Cameroon, electricity of France and the energy of Cameroon (ENEO). These data were collected on a daily time step. The choice of these data is due to the regulated nature of the basins and the difficulty of obtaining information on their management to configure the model in such a way as to take regulation into account. Ignoring the regulation, we considered the natural state of the basin and calibrated the model produced with the naturalized flows.

2.2.2. Assessment of the impact of climate variability (CV) and land use and land cover changes (LULCCs) on water resources

2.2.2.1. Design of numerical simulation. Since the study includes a historical period or baseline (BL) (2002–2019) and two future periods, P1 (2024–2035) and P2 (2036–2050), to find out whether forcings (CV and LULCCs) have an impact on the evolution of WBCs (groundwater recharge: GW_RCH; runoff: SURQ; potential evapotranspiration: PET and water yield: WYLD) in the basins studied, we considered the following climate and LULC evolution scenarios:

3. The combined impact of the two forcings on WBCs

In this case, the LULC maps of 2010, 2030 and 2040 were respectively used to simulate the flows of the historical period (BL), P1 and P2. The mean values of the WBCs of P1 and P2 were compared to those of BL according to the equation:

$$\Delta WBC_{Pi} = WBC_{Pi} - WBC_{BL} \quad (1)$$

Where ΔWBC_{Pi} is the change between the WBC value of the corresponding period ($Pi = P1$ or $P2$) and that of the BL; WBC_{Pi} is the WBC value of the corresponding period, and WBC_{BL} is the WBC value of the BL.

4. The unique impact of CV on WBCs

To assess the impact of CV only, LULC is considered to have experienced no change during P1 and P2. It therefore remained identical to those of the BL. The equation used for this calculation is:

$$\Delta WBC_{CLi} = WBC_{CLiPi} - WBC_{BL} \quad (2)$$

Where ΔWBC_{CLi} is the change between the WBC value of the corresponding period ($Pi = P1$ or $P2$) and that of the BL; WBC_{CLiPi} is the WBC value of the corresponding period, and WBC_{BL} is the WBC value of the BL.

5. The unique impact of LULCCs on WBCs

To assess the impact of LULCCs only, we considered that meteorological data of P1 and P2 are identical to those of the BL. The only forcing that changed here is LULC. The equation used for this calculation is:

$$\Delta WBC_{Li} = WBC_{LiPi} - WBC_{BL} \quad (3)$$

Where ΔWBC_{Li} is the change between the WBC value of the corresponding period ($P_i = P1$ ou $P2$) and that of the BL; WBC_{LiPi} is the WBC value of the corresponding period, and WBC_{BL} is the WBC value of the BL.

5.1. Impact score of LULCCs and CV on WBCs

To know which is the forcing whose impact is predominant in the WBCs, the impact scores of LULCCs and CV were calculated according to the method of [Bennour et al. \(2023\)](#).

$$CR_WBC_{CLi} = \Delta WBC_{CLi} / \Delta WBC \quad (4)$$

$$CR_WBC_{Li} = \Delta WBC_{Li} / \Delta WBC \quad (5)$$

Where CR_WBC_{CLi} and CR_WBC_{Li} are the respective scores of the impact of CV and LULCCs on WBCs. ΔWBC , ΔWBC_{CLi} and ΔWBC_{Li} were calculated by [Eqs. \(1\), \(2\) and \(3\)](#). High scores indicate a dominant impact.

5.1.1. Modeling changes in LULC patterns

Future LULC was predicted using the CA-Markov procedure. This procedure is also described as “cellular automata” (CA) ([Halmy et al., 2015](#)). Markovian chains analyze two images of LULC at different years and produce two transition matrices (probability and affected area in pixels for persistence and transition), and a set of conditional probability images. They make it possible to calculate a future state from a well-known present state, based on the observation of past evolutions and their probability. This makes this method one of the best for modelling both temporal and spatial dimensions of LULC ([Halmy et al., 2015; Yang et al., 2019](#)).

The Kappa coefficients calculated by the following equation allowed us to evaluate the performance of the CA-Markov model in predicting LULC:

$$Kappa = \frac{Po - Pc}{1 - Pc} \quad (6)$$

Where Po is the proportion of correctly simulated cells; Pc is the expected proportion correction by chance between the observed and simulated map. When the Kappa coefficient ≤ 0.5 , this indicates poor proximity between the two compared maps (simulated and observed). When $0.5 \leq Kappa \leq 0.75$, the proximity between the two maps is acceptable. If $0.75 \leq Kappa \leq 1$, the proximity between the two maps is good. A Kappa coefficient = 1 indicates that the two maps are identical. The Kappa coefficient obtained for the comparison between the observed and simulated maps for the year 2015 in this study is 0.89, which gives credibility to the simulated maps for the years 2030 and 2040.

5.1.2. Climate change scenarios

In this study, four (04) regional climate models (RCMs) (high resolution limited area model, version 5:HIRHAM5; regional model: REMO; Rossby centre regional atmospheric model, version 4: RCA4 and canadian centre for climate modelling and analysis: CCCma) from the CORDEX (coordinated regional climate downscaling experiment) project, proven to be effective in simulating precipitation and temperature in Africa ([Gadissa et al., 2018; Dibaba et al., 2019](#)), were retained. For each of the RCMs, data from the RCP4.5 and RCP8.5 scenarios were collected. The first and second scenarios are respectively representative of moderate and high greenhouse gas emissions. The other meteorological variables (solar radiation, relative humidity and wind speed) considered for the historical period have been taken over for the two future periods without making any changes, given that their modifications have no significant impact on the modelling result ([Gadissa et al., 2018](#)).

5.1.3. Bias correction

Despite their reliability and the degree of confidence that can attributed to RCMs data, they sometimes present considerable biases. It therefore become necessary to correct them before evaluating the impact of climate change. climate model data for hydrological modeling (CMhyd) software ([Rathjens et al., 2016](#)) obtained from: <https://swat.tamu.edu/software/> was used to correct for precipitation and temperature biases. A comprehensive review of bias correction techniques based on this tool was provided by some authors ([Teutschbein and Seibert, 2012; Zhang et al., 2018](#)). According to them, all the correction techniques improved the simulations of precipitation and temperature. However, they noted differences among the correction methods. Based on the proximity between the corrected and the observed datasets, distribution mapping (DM) was considered as the best correction method both for temperature and precipitation. According to the authors, distribution mapping uses a transfer function to adjust the cumulative distribution of the corrected data to that of the observed data, which makes the results significantly better. Based on these results, we retained distribution mapping for the precipitation and temperature corrections of the RCMs data in this study.

5.1.4. Model description

SWAT is a physically based semi-distributed hydrological model, designed and developed by researchers at the USDA (United States Department of Agriculture) (Arnold et al., 1998). Its physical aspect allows us to reproduce the processes that really take place in the environment, using a different set of equations (Neitsch et al., 2005; Arnold et al., 2012). The SWAT model is continuous over time and is designed to run simulations over long periods (Payraudeau, 2002). This model analyzes the watershed as a whole by subdividing it into sub-watersheds containing homogeneous portions called hydrological response units (HRUs). Each HRU is characterized by a unique land use, soil type and topography. SWAT provides the different WBCs at the HRU scale over the simulation period (Neitsch et al., 2005).

5.1.5. Model evaluation criteria

The validity of the SWAT model was checked by comparing the simulated (Q_{sim}) and observed (Q_{obs}) flows through subjective and quantitative criteria. Initially, a good match between the observed and simulated flow hydrographs will attest to good calibration. In the second step, we used four (04) of the most widely used criteria for the validation of hydrological models: coefficient of determination (R^2), Nash-Sutcliffe efficiency (NSE), Kling-Gupta efficiency (KGE) and the percent bias (PBIAS) (Akoko et al., 2020). According to Moriasi et al. (2007), $NSE \geq 0.5$ are acceptable. A KGE and $R^2 \geq 0.5$ are also acceptable according to Akoko et al. (2020).

$$R^2 = \frac{\sum_{i=1}^n (Q_{obs,i} - \bar{Q}_{obs})(Q_{sim,i} - \bar{Q}_{sim})}{\sqrt{(\sum_{i=1}^n (Q_{obs,i} - \bar{Q}_{obs})^2)(\sum_{i=1}^n (Q_{sim,i} - \bar{Q}_{sim})^2)}} \tag{7}$$

$$NSE = 1 - \frac{\sum (Q_{sim} - Q_{obs})^2}{\sum (Q_{obs} - \bar{Q}_{obs})^2} \tag{8}$$

$$KGE = 1 - \sqrt{(r - 1)^2(\alpha - 1)^2(\beta - 1)^2} \tag{9}$$

$$PBIAS = 100 \frac{\sum_{i=1}^N (Q_{est,i} - Q_{obs,i})}{\sum_{i=1}^N Q_{obs,i}} \tag{10}$$

Where Q_{obs} is the observed flow for time step i ; Q_{sim} is the simulated flow for time step i ; \bar{Q}_{obs} is the average of the observed flows; \bar{Q}_{sim} is the average of the simulated flows; n is the number of observations; r is the Pearson correlation coefficient between observed and simulated flows; α is the standard deviation of simulated flows and β is the ratio of the mean simulated flows.

6. Results and discussion

6.1. SWAT model performance

To identify the parameters having a significant influence on the model outputs, a sensitivity analysis was carried out based on the average monthly flows observed. Nine (09) parameters appeared to be the most sensitive for the calibration (Table 2). These parameters are essentially related to infiltration, hydraulic conductivity, evaporation, etc.

Regarding the results of the SWAT model, they are overall satisfactory. A good agreement is observed between observed and simulated flows for the two basins (Figs. 5 and 6). In calibration and validation, this good performance is materialized by R^2 , NSE and KGE greater than 0.68. Bias $\pm 10\%$ also attests to this good performance (Fig. 5).

Table 2
Sensitivity analysis and calibrated parameters.

Parameters	Description	t-Stat		P-Value		Sensitivity rank		Parameter value range		Fitted value	
		Mba	Bam	Mba	Bam	Mba	Bam	Min	Max	Mba	Bam
9:V_CH_K2.rte	Effective hydraulic conductivity in the main channel (mm hr ⁻¹)	-0.007	0	0.995	1	1	6	5	130	101.6	0.82
1:R_CN2.mgt	SCS runoff curve number for moisture condition II	0.010	0.002	0.993	0.999	2	3	-0.2	0.2	0.1	0.23
4:V_GWQMN.gw	Threshold depth of water in the shallow aquifer required for return flow to occur (mm)	-0.015	-0.002	0.991	0.999	3	1	0	2	0.8	0.11
7:R_SOL_AWC(.).sol	Available water capacity of the soil layer (mm H ₂ O/mm)	0.024	-0.007	0.985	0.996	4	4	-0.2	0.4	-0.1	-0.06
2:V_ALPHA_BF.gw	Base flow alpha factor (days)	0.050	0.007	0.968	0.995	5	9	0	1	0.9	430.91
5:R_EPCO.bsn	Plant uptake compensation factor	-0.064	0.007	0.959	0.995	6	2	0	1	0.2	101.59
6:V_ESCO.hru	Soil evaporation compensation factor	0.118	0.010	0.925	0.993	7	8	0.8	1	0.8	0.73
3:V_GW_DELAY.gw	Groundwater delay (days)	0.155	-0.012	0.902	0.992	8	5	30	450	430.9	0.83
8:R_SOL_K(.).sol	Saturated hydraulic conductivity (mm hr ⁻¹)	0.195	-0.017	0.877	0.989	9	7	-0.8	0.8	0.7	0.86

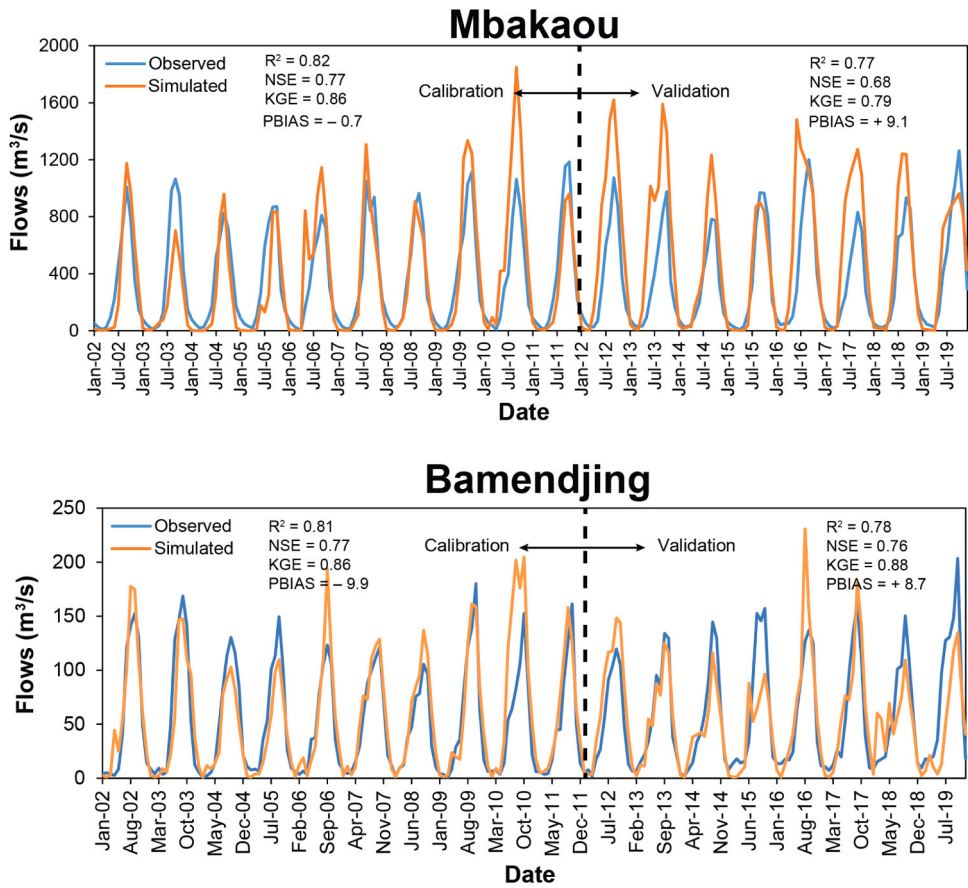


Fig. 5. Calibration (2002–2011) and validation (2012–2019) of average monthly flows.

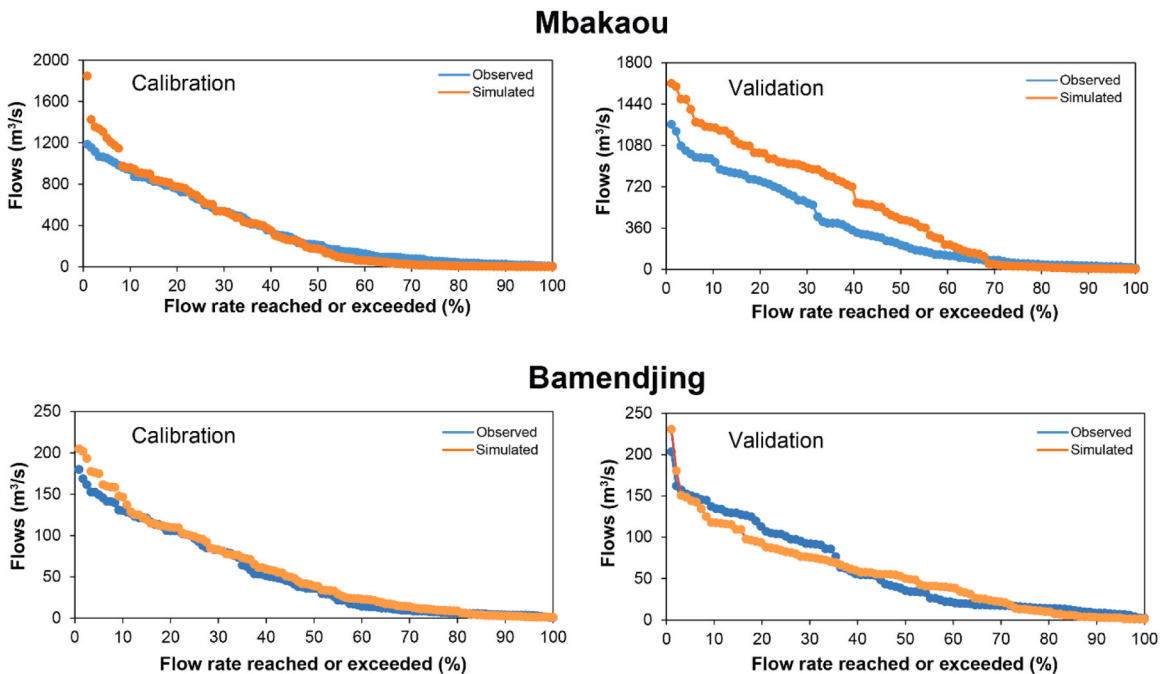


Fig. 6. Observed and simulated monthly flow-duration curves for calibration and validation.

Looking at the spatial distribution of water balance elements (WBCs) (flows: SURQ, groundwater recharge: GW_RCH, potential evapotranspiration: PET and water yield: WYLD), flows and sediment yield (SED), we generally realize that in both basins, GW_RCH, flows, WYLD and SED are greater in the middle zone. Conversely, SURFQ is low in this part of the basins (Fig. 7). This seems to be related to the configuration of the relief, which seems lower and less rugged in the middle zone of the said basins (Figs. 3D and 4D). As

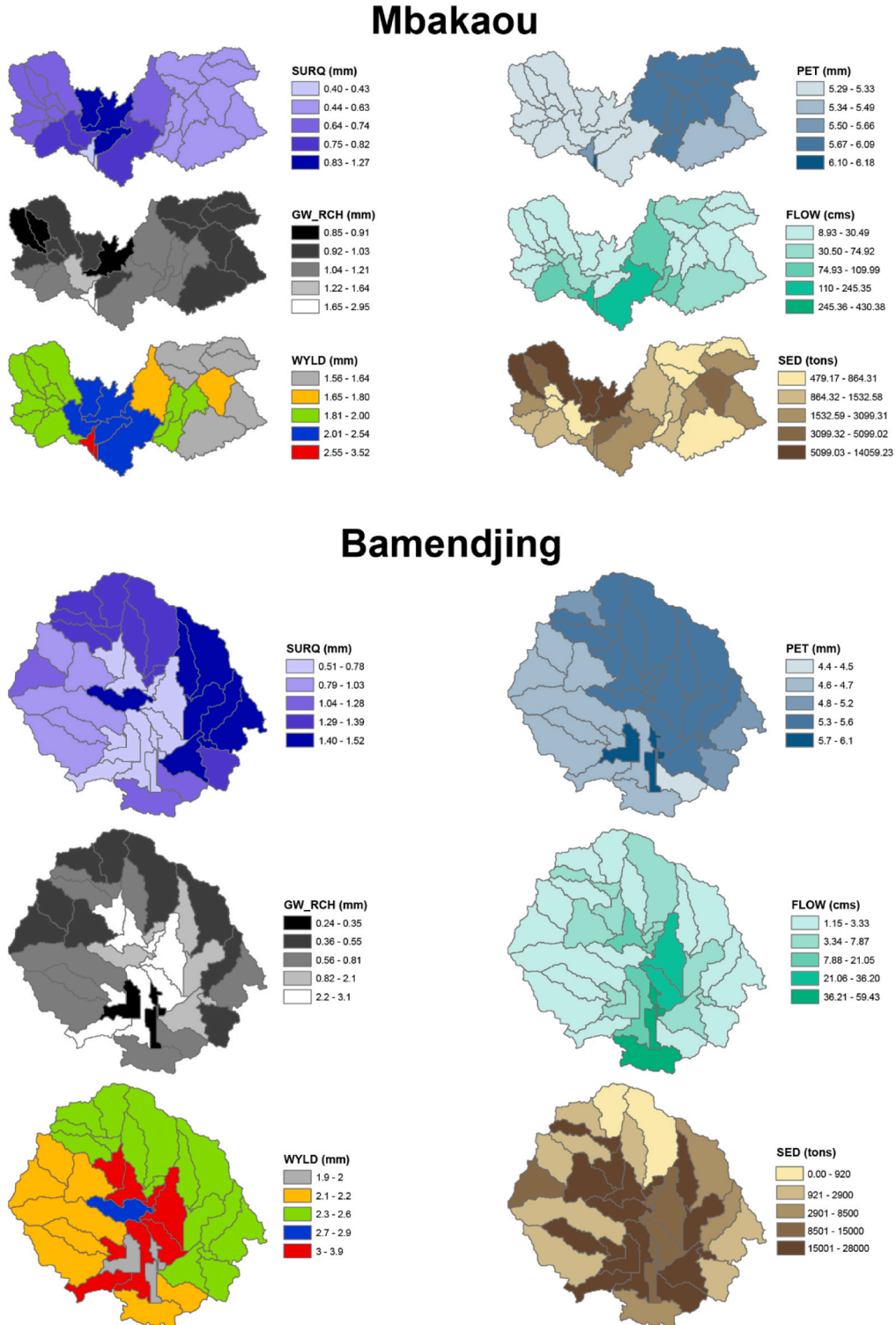


Fig. 7. Spatial distribution of water balance components (SURQ, PET, GW_RCH and WYLD), flows and sediments load.

for PET, it seems to be greater to the East of the basins (Fig. 7), probably due to the higher temperatures in this part.

The SWAT model has already been successfully calibrated in Central Africa. Ebodé (2023) successfully calibrated and validated this model in the case of the Nyong basin at the Mbalmayo gauging station. This was done for two different periods, considering land use and land cover (LULC) (1981–1986 and 2009–2014). For the first and the second period, R^2 and NSE respectively greater than 0.80 and 0.64 were obtained in calibration and validation.

6.2. Future hydroclimatic variability

6.2.1. Future evolution of the climate according to the RCMs

To assess future climate change, the average precipitation and temperature of each model (CCCma, HIRHAM 5, RCA4, REMO and ENS), each emission scenario (RCP 4.5 and RCP 8.5) and each period (2024–2035 and 2036–2050) were compared to those of the historical period/baseline (BL) (2002–2019).

6.2.1.1. Predicted rainfall. Compared to the historical period, two models (CCCma and REMO) predict in the near future (2024–2035) a decrease in precipitation and two (HIRHAM5 and RCA4) others predict the opposite, whatever the basin (Mbakaou or Bamendjing) and the emission scenario considered (RCP8.5 or RCP4.5) (Tables 3 and 4; Fig. 8). The intensity of the decline predicted by the CCCma model is greater for the Mbakaou basin. This model forecasts declines of –35.4% and –25.6, respectively for the RCP8.5 and RCP4.5 scenarios. In the case of Bamendjing, it is rather the REMO model that predicts the largest decline. For these same scenarios, the reductions envisaged are respectively –17.2% and –16.2% (Table 3). The HIRHAM5 model forecasts a greater increase in precipitation than the RCA4 model over the two basins. The increases predicted by the HIRHAM5 model for the first and second scenarios in the Mbakaou basin are 74.2% and 85.2%, respectively (Table 3). For these scenarios, the increases envisaged in the Bamendjing basin are 29.2% and 31.8% (Table 3). Overall, an increase in precipitation is expected in both basins. In the Mbakaou basin, the projected increases for the RCP8.5 and RCP4.5 scenarios are 17.1% and 22.2%. For the same scenarios, the increases in rainfall forecast in the Bamendjing basin are lower, 7.5% and 8.6% respectively (Table 3).

During the second future period (2036–2050), we note the same trends as in the first period (Tables 3 and 4; Fig. 9). However, we note a slight amplification of the increases and decreases identified in the various cases, with the exception for the HIRHAM5 model, for which the intensity of the decrease is attenuated in both basins (Table 3). The decreases and increases noted during the first and second periods mainly concern the months of the rainy season (March–November) (Figs. 8 and 9).

These results present similarity and divergence points with studies carried out in Africa using the same models. In the Finchaa basin in Ethiopia, Dibaba et al. (2020) highlighted a decrease in precipitation over the future period from the RCA4 model. This study, however, predicts the opposite evolution of rainfall from the outputs of the same model. This study highlights a decrease in precipitation from the CCCma model over the future period. Ebodé (2023) obtained an identical result in his study conducted in a neighbouring basin of the Sanaga (Nyong).

6.2.1.2. Predicted temperatures. Referring to the historical period, all models (CCCma, HIRHAM5, RCA4 and REMO) predict an

Table 3

Projected changes (%) in rainfall, maximum temperatures, minimum temperatures and flows for the different periods, models and scenarios compared to baseline period.

Models and scenarios	First period (2024–2035)				Second period (2036–2050)			
	Rainfall	TMPMAX	TMPMIN	Flows	Rainfall	TMPMAX	TMPMIN	Flows
Mbakaou								
REMO_RCP8.5	-14.2	1.9	0.9	-6.1	-19.0	2.3	1.5	-18.0
REMO_RCP4.5	-14.5	1.7	0.7	-8.9	-17.5	2.1	1.1	-15.1
RCA4_RCP8.5	25.7	2.1	1.0	88.3	37.1	2.7	1.6	113.5
RCA4_RCP4.5	29.7	2.0	0.9	100.5	29.6	2.4	1.1	96.9
HIRHAM5_RCP8.5	74.2	2.2	8.4	228.7	70.2	3.0	8.9	219.9
HIRHAM5_RCP4.5	85.2	1.9	8.1	255.5	83.4	2.8	8.1	254.1
CCCma_RCP8.5	-35.4	2.2	1.0	-38.7	-41.0	2.9	1.6	-38.7
CCCma_RCP4.5	-25.6	2.0	0.8	-18.2	-39.0	2.4	1.3	-45.9
ENS_RCP8.5	17.1	2.1	2.8	57.1	16.3	2.7	3.4	53.2
ENS_RCP4.5	22.2	1.9	2.6	70.6	17.5	2.4	3.1	58.8
Bamendjing								
REMO_RCP8.5	-17.2	0.9	0.7	-26.1	-14.9	1.1	1.2	-20.8
REMO_RCP4.5	-16.8	0.8	0.4	-23.1	-20.2	1.0	0.9	-30.6
RCA4_RCP8.5	10.9	1.1	1.0	39.8	20.9	1.6	1.6	59.3
RCA4_RCP4.5	14.4	1.0	0.5	48.1	14.3	1.3	0.7	47.5
HIRHAM5_RCP8.5	29.2	3.7	9.4	54.0	26.8	4.3	9.8	49.2
HIRHAM5_RCP4.5	31.8	3.5	9.2	61.1	27.8	3.5	9.6	51.0
CCCma_RCP8.5	-8.3	1.3	0.5	-21.0	-12.4	1.8	0.9	-28.8
CCCma_RCP4.5	-10.8	1.1	0.4	-12.8	-13.2	1.4	0.6	-15.1
ENS_RCP8.5	7.5	1.7	2.9	6.7	9.0	2.2	3.4	10.2
ENS_RCP4.5	8.6	1.6	2.6	11.8	6.1	2.0	3.0	6.2

Table 4
 Projected changes (%) in rainfall, maximum temperatures, minimum temperatures and flows for the different pentads, models and scenarios compared to baseline period.

Basins	Mbakaou										Bamendjing									
	CCCma		HIRHAM5		RCA4		REMO		ENS		CCCma		HIRHAM5		RCA4		REMO		ENS	
Scenario	RCP4.5	RCP8.5	RCP4.5	RCP8.5	RCP4.5	RCP8.5	RCP4.5	RCP8.5	RCP4.5	RCP8.5	RCP4.5	RCP8.5	RCP4.5	RCP8.5	RCP4.5	RCP8.5	RCP4.5	RCP8.5	RCP4.5	RCP8.5
Rainfall (%)																				
2024–2025	-29.7	-12.4	48.3	73.4	24.5	14.7	-11.5	-14.8	11.4	19.8	-4.5	-7.9	45.5	30.8	9.8	1.1	-15.2	-18.3	12.9	5.1
2026–2030	-24.6	-43.9	84.5	73	29.1	27.7	-11.9	-12.1	22.8	15.7	-9.2	-8	27	27.4	13.8	12.6	-16.5	-13.8	7.7	8.5
2031–2035	-25	-36.1	100.7	75.7	32.3	28.2	-18.3	-16	25.9	17.5	-14.8	-8.7	31.2	30.5	16.7	13.1	-17.7	-20.3	7.8	7.4
2036–2040	-44.2	-41.9	77.6	64.9	38.6	28.5	-21.3	-23.4	16.1	11.4	-3.5	-13.9	26.8	28.2	22.3	13.4	-20.1	-12	10.5	7.7
2041–2045	-29.4	-37.9	94.8	81.5	22.8	38.8	-17.2	-15.3	21.1	21.3	-17.3	-11.7	28.4	26	8.3	22.4	-19.4	-15.6	3.8	9.2
2046–2050	-43.2	-43.2	77.9	64	27.3	43.9	-14	-18.2	15.4	16.1	-18.7	-11.5	28.2	26.3	12.3	26.9	-21	-17	4.1	10.1
TMPMAX (°C)																				
2024–2025	2.0	1.8	1.5	1.8	2.4	1.8	1.9	1.9	1.9	1.8	1.0	1.1	3.3	3.4	1.0	0.9	0.8	0.8	1.5	1.6
2026–2030	2.0	2.0	1.7	2.0	1.9	2.3	1.6	1.9	1.8	2.1	1.0	1.1	3.5	3.6	1.0	1.2	0.7	0.9	1.5	1.7
2031–2035	2.1	2.6	2.1	2.5	1.9	2.1	1.9	1.9	2.0	2.3	1.3	1.6	3.7	4.0	1.1	1.1	0.9	0.9	1.7	1.9
2036–2040	2.4	2.6	2.5	2.2	2.1	2.5	1.8	2.0	2.2	2.3	1.4	1.5	3.9	3.8	1.0	1.7	0.9	1.0	1.8	2.0
2041–2045	2.2	2.9	3.1	3.0	2.6	2.8	2.1	2.3	2.5	2.7	1.5	1.9	4.3	4.3	1.4	1.7	1.0	1.2	2.0	2.3
2046–2050	2.4	3.1	3.0	3.7	2.6	2.7	2.3	2.4	2.5	2.9	1.4	2.0	4.1	4.8	1.4	1.6	1.1	1.2	2.0	2.4
TMPMIN (°C)																				
2024–2025	0.7	0.8	7.9	8.2	1.0	0.8	1.0	0.6	2.6	2.6	-1.8	-1.7	7.0	7.2	-1.4	-1.5	-1.4	-1.6	0.6	0.6
2026–2030	0.9	0.9	7.9	8.2	0.8	1.0	0.6	1.0	2.5	2.8	0.6	0.4	9.1	9.2	0.5	1.0	0.4	0.8	2.6	2.9
2031–2035	0.9	1.2	8.3	8.6	0.9	1.1	0.7	1.1	2.7	3.0	0.3	0.6	9.3	9.5	0.4	1.0	0.4	0.8	2.6	3.0
2036–2040	1.3	1.2	8.6	8.4	1.0	1.7	0.9	1.3	2.9	3.1	0.6	0.7	9.4	9.4	0.6	1.5	0.8	1.0	2.9	3.1
2041–2045	1.2	1.6	9.0	8.9	1.3	1.6	1.4	1.5	3.2	3.4	0.6	0.9	9.7	9.8	0.9	1.6	1.0	1.2	3.0	3.4
2046–2050	1.3	1.8	8.9	9.4	1.2	1.6	1.1	1.6	3.1	3.6	0.7	1.1	9.6	10.1	0.7	1.7	0.89	1.3	3.0	3.5
Flows (%)																				
2024–2025	-27.6	9.6	158	218.9	87.9	62.5	-8.5	-5.8	37.3	66.3	-2.4	-20	82.2	63.4	40.1	24.2	-20.5	-23.3	16.3	5
2026–2030	-18.9	-55.2	250.5	223.1	96.3	91.3	-7.3	-4.7	69.7	51.2	-13.5	-21.1	53	45.5	46.3	41.6	-23.8	-19.6	8.8	6.7
2031–2035	-13.7	-41.5	299.6	238.3	109.8	95.5	-10.6	-7.6	84.9	59.4	-16.2	-21.4	60.7	58.7	53	44.1	-23.4	-33.8	13	7.3
2036–2040	-57.2	-48.8	244.4	212.5	121.2	99.7	-18.6	-22.6	59.3	47.3	2.4	-29.7	50.1	50.5	62.8	45.3	-28.9	-13.8	15.6	7.2
2041–2045	-24.4	-50.9	280	242.5	73.7	112.4	-22.8	-15.6	62.5	59.7	-19.9	-27.1	53.9	50.9	37.2	64.1	-29.6	-22.6	2.5	13.2
2046–2050	-56.1	-55.3	238	204.7	95.6	128.4	-3.8	-15.8	54.5	52.7	-27.9	-29.6	48.9	46.2	42.4	68.7	-33.3	-26.1	0.5	10.3

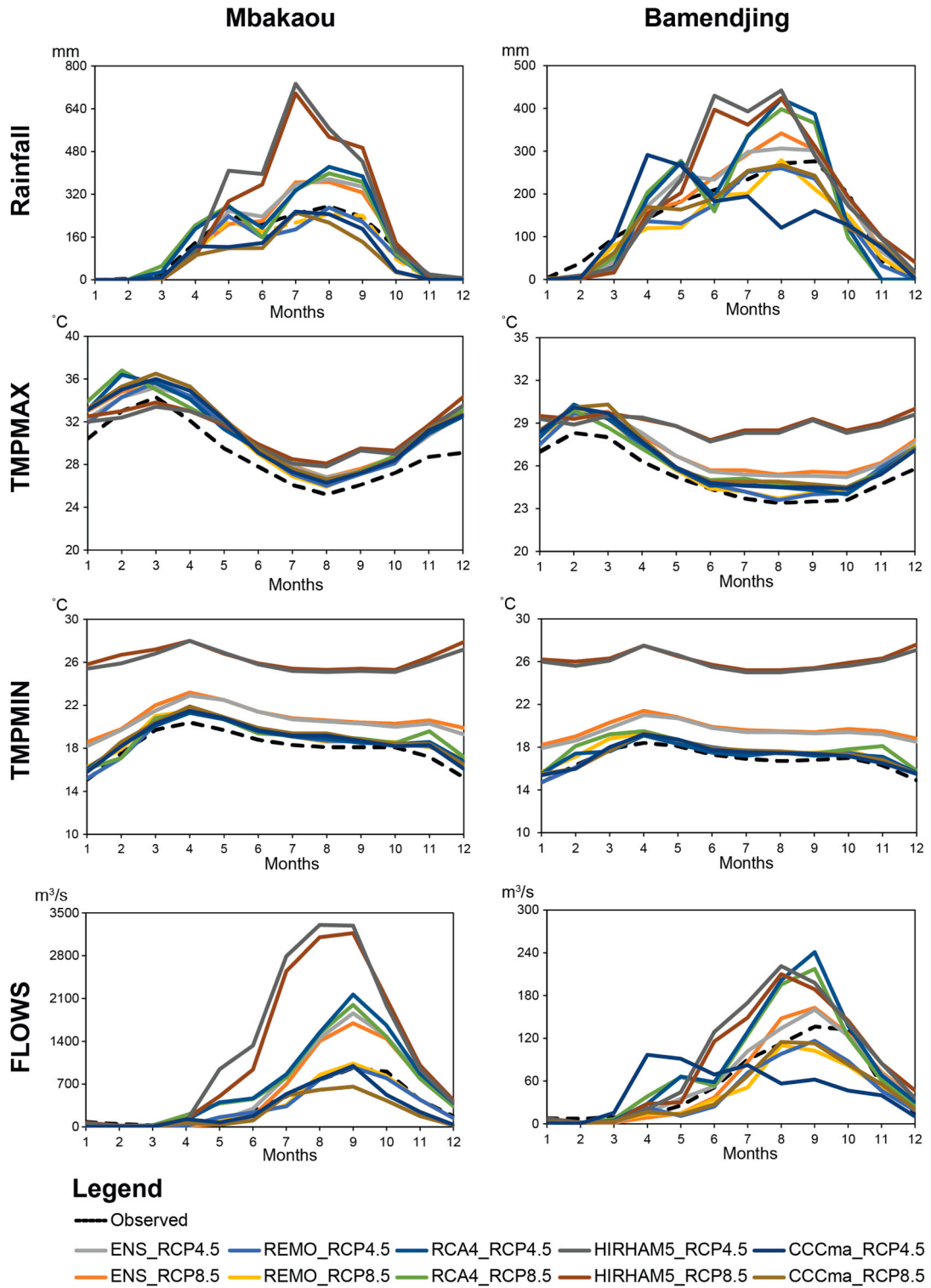


Fig. 8. Projected changes (compared to baseline period) in monthly/seasonal mean rainfall, maximum temperatures, minimum temperatures and flows for the first period (2024–2035) under the RCP4.5 and RCP8.5 scenarios.

increase in maximum and minimum temperatures during the two future periods (2024–2035 and 2036–2050) (Tables 3 and 4; Figs. 8 and 9). The HIRHAM5 model predicts the largest increases. For maximum temperatures, the projected increases for the RCP8.5 and RCP4.5 scenarios are 2.2°C and 1.9°C, respectively in the Mbakaou basin during the first period. In the Bamendjing basin, the increases

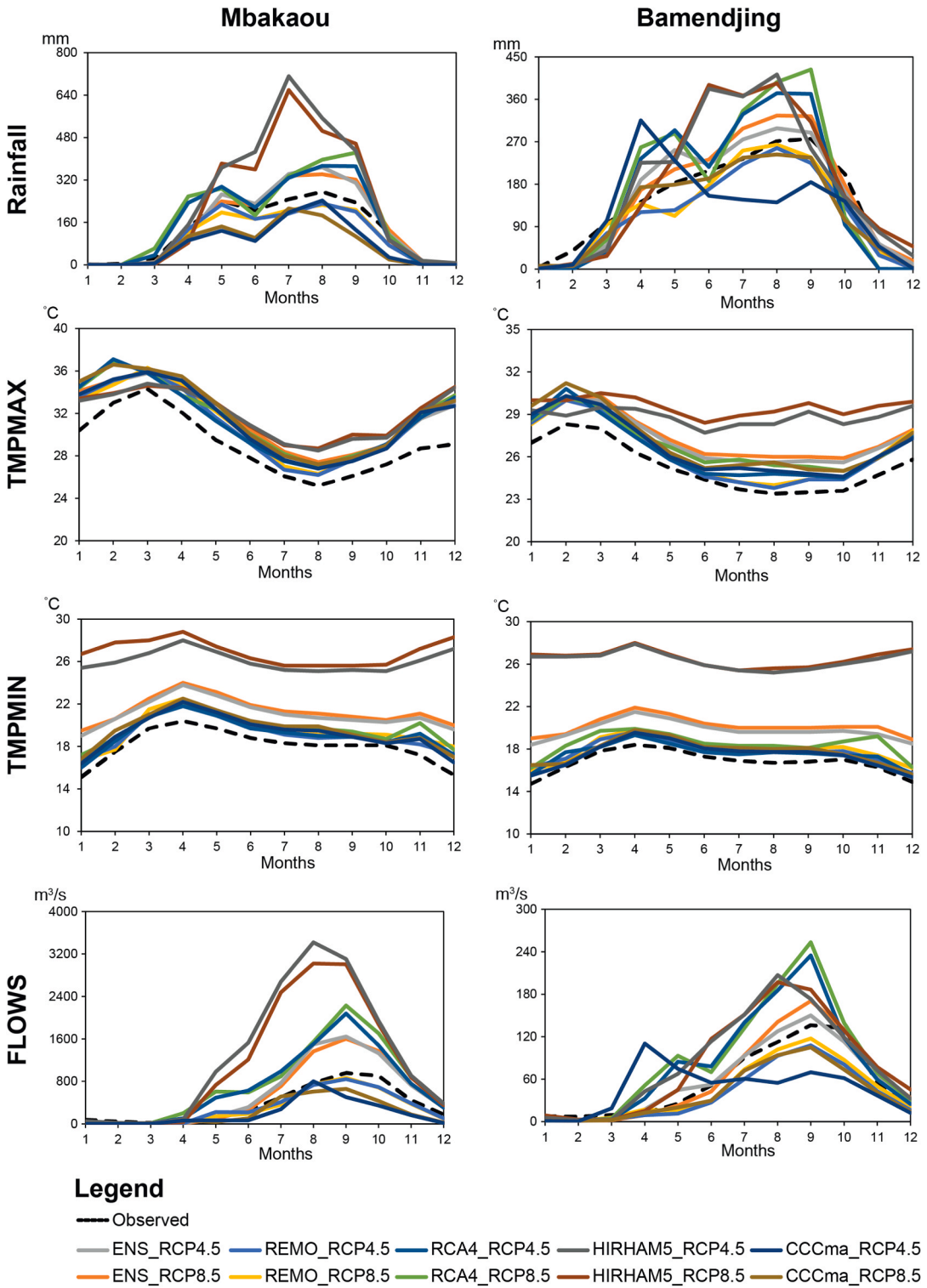


Fig. 9. Projected changes (compared to baseline period) in monthly/seasonal mean rainfall, maximum temperatures, minimum temperatures and flows for the second period (2036–2050) under the RCP4.5 and RCP8.5 scenarios.

predicted for the same period and scenarios are 3.7°C and 3.5°C (Table 3). For minimum temperatures, the increases predicted by the HIRHAM5 model in the Mbakaou basin for the RCP8.5 and RCP4.5 scenarios are 8.9°C and 8.1°C during the second period (Table 3). In the Bamendjing basin, the projected increases for the same period and scenarios are similar (9.8°C and 9.6°C) (Table 3). All models

predict a gradual increase in maximum and minimum temperature over the pentads (period of five years) with maximum values during the last two pentads (2041–2045 and 2046–2050) (Table 4).

As is the case in this work, several other studies on similar themes have already shown a gradual rise in maximum and minimum temperatures over time (Kingston and Taylor, 2010; Basheer et al., 2015; Koffi et al., 2023).

6.2.1.3. Predicted flows. Forecasts from climate models (rainfall and temperature) were integrated into the SWAT model to simulate future flows in both watersheds. The runoff trends during the two periods (2024–2035 and 2036–2040) are identical to those of the precipitation outputs used in the model, which suggests a strong annual rainfall-runoff relationship in the investigated basins. Thus, a change in precipitation consistent with the predictions of the CCCma and REMO models will cause a decrease in runoff, while a change in precipitation consistent with the predictions of the RCA4 and HIRHAM 5 models will cause an increase (Table 3). During the first future period (2024–2035), the declines in runoff simulated from the precipitation of the CCCma model are the most significant in the Mbakaou basin. They are -38.7% and -18.2% for the RCP8.5 and RCP4.5 scenarios. In the Bamendjing basin, it is the decreases in runoff simulated from the precipitation of the REMO model that are the most significant -26.1% and -23.1% for the RCP8.5 and RCP4.5 scenarios respectively (Table 3). The increases in flows simulated from the precipitation of the HIRHAM5 model are greater in

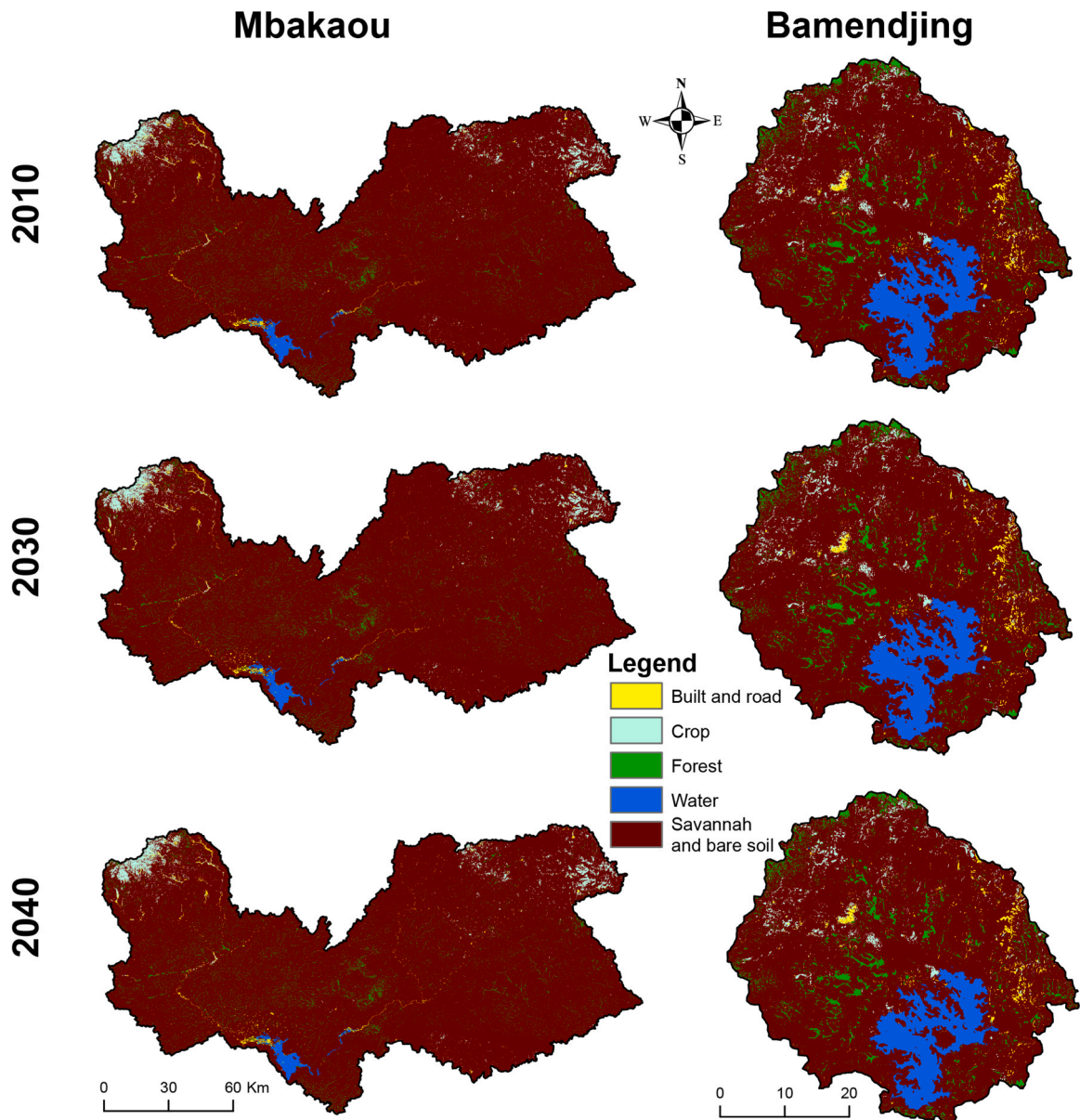


Fig. 10. Land use map of 2010, and predictive land use maps of 2030 and 2040.

the two basins. In the case of Mbakaou, they are 228.7% and 255.5% for the RCP8.5 and RCP4.5 scenarios. For these same scenarios, they are 54% and 61% in the case of Bamendjing.

During the second future period (2036–2050), identical trends to those of the first period are noted in the evolution of flows (Tables 3 and 4; Fig. 9). It should nevertheless be noted a slight amplification of increases and decreases in the different cases, except for the HIRHAM5 model, for which the intensity of the decrease noted is lessening in the two basins (Table 3). The trends (decreases and increases) noted during the first and second periods mainly concern the months of the rainy season (March–November) (Figs. 8 and 9).

To get an idea of the future evolution of water resources, several authors have integrated climate model forecasts into hydrological models (Notter et al., 2013; Wagena et al., 2016; Danvi et al., 2018; Duku et al., 2018). As is the case in this study, some of these works predict an evolution of flows identical to that of precipitation (Beyene et al., 2010; Basheer et al., 2015; Dibaba et al., 2020).

6.3. Future evolution of LULC

Five land use and land cover (LULC) classes having a direct link to runoff have been identified in the studied basins (Built and road, savannah and bare soil, crop, water and forest) (Fig. 10). The LULC forecasts for the years 2030 and 2040 were made based on the evolution recorded between 1984 and 2010. The 2010 map serves as a reference. It is the one against which future changes are assessed.

Relatively small changes overall are projected for future periods (Fig. 10). Between 2010 and 2030, a slight increase in buildings, bare soils and crops is expected in the two basins. In the case of Mbakaou, the growth rates recorded are 0.9%, 0.005% and 0.5%, respectively. In that of Bamendjing, the evolution rates recorded are 1.8%, 0.1% and 1.1% (Table 5). Over this interval, it is conversely expected in these basins a slight decrease in forest and water bodies. The respective rates of change recorded in the Mbakaou basin are –0.7% and –0.4%. In the Bamendjing basin, these rates are respectively –0.3% and –3.3% (Table 5). Between 2010 and 2040, the projected changes are almost identical to those of the period 2010–2030 (Table 5).

Projected land use and land cover changes (LULCCs) in the basins studied are very low overall. This could be related to the fact that these basins are almost entirely covered with savannah. The area of forest in these basins is very small. However, it is the LULC type that is most subject to anthropogenic pressure in the region (Ebodé et al., 2020, 2022). In the event of absence, as is the case in the basins studied, LULC remains practically static. Moreover, it is foreseeable that such slight changes will have a very limited impact on future flows.

6.4. Impact of CV and LULCCs on WBCs

Table 6 presents the changes in the different WBCs (SURQ, GW_RCH, PET and WYLD) according to the possible evolution scenarios (LULCCs & CV, CV, LULCCs). We note that whatever the model (CCCma, HIRHAM5, RCA4 and REMO) and the emission scenario (RCP4.5 and RCP8.5) considered, the variables describing the WBCs change significantly for the LULCCs & CV scenarios and CV. The trend observed for PET is similar to that of temperatures (increase). The trends of the other three variables are generally consistent with those of precipitation (decrease for the CCCma and REMO models, and increase for the HIRHAM5 and RCA4 models) (Table 6). We also note that for all the models, the change observed in the different variables of the hydrological balance is low for the LULCCs evolution scenario, 1% in all cases (Table 6).

Similarly, by looking at Table 7, which presents the scores for the future impact of CV and LULCCs on the four (04) WBCs retained, we see that the scores for the impact of CV are higher than those for LULCCs. Regardless of the model, future period (2024–2035 or 2036–2050) and emission scenario (RCP4.5 or RCP8.5) taken into account, the scores for the impact of CV on different WBCs are equal to 1. However, the score of the impact of LULCCs are all less than 0.09 (Table 7). All this suggests that CV will be the dominant forcing of future flows in the investigated basins.

Several authors around the world are already interested in separating the impact of CV and LULCCs on water resources (Bennour et al., 2023). As is the case in this work, others have highlighted in East Africa the preponderant impact of CV on the evolution of water resources (Dibaba et al., 2020).

Table 5
Statistics for land use map of 2010 and simulated land use maps (2030 and 2040).

Land-use modes	Mbakaou					Bamendjing				
	2010	2030	2040	Change 2010–2030	Change 2010–2040	2010	2030	2040	Change 2010–2030	Change 2010–2040
Built and road	111	112	113.5	0.9	2.3	27.5	28	29	1.8	5.5
Bare soil, savannah and young fallow	18855	18856	18858	0.005	0.02	1813	1814	1814.5	0.1	0.1
Crop	406	408	409	0.5	0.7	46	46.5	47	1.1	2.2
Water body	142	141	141	-0.7	-0.7	200	199	199	-0.3	-0.3
Forest and old fallow	790	787	782.5	-0.4	-0.9	120	117.5	115.5	-1.7	-3.3

Table 6
Projected changes (%) in water balance components for the different experiments, periods, models and scenarios compared to baseline period.

Periods	Models	PET			SURQ			GW_RCH			WYLD		
		LULCC&CV	CV	LULCC	LULCC&CV	CV	LULCC	LULCC&CV	CV	LULCC	LULCC&CV	CV	LULCC
Mbakaou													
P1	CCCma_RCP4.5	11.3	11.3	1	4.9	4.9	1	-22.1	-22.1	1	-18.4	-18.4	1
	CCCma_RCP8.5	12.4	12.4	1	-0.2	-0.2	1	-26.3	-26.3	1	-28	-28	1
	HIRHAM5_RCP4.5	31.5	31.5	1	64	64	1	43.1	43.1	1	109.6	109.6	1
	HIRHAM5_RCP8.5	33.5	33.5	1	55.9	55.9	1	38.9	38.9	1	97.1	97.1	1
	RCA4_RCP4.5	11.6	11.6	1	12.6	12.6	1	23	23	1	37	37	1
	RCA4_RCP8.5	12.3	12.3	1	11	11	1	19.1	19.1	1	31.3	31.3	1
	REMO_RCP4.5	9.9	9.9	1	-2.9	-2.9	1	-10.5	-10.5	1	-14	-14	1
	REMO_RCP8.5	11.5	11.5	1	-3.1	-3.1	1	-9.1	-9.1	1	-12.7	-12.7	1
	ENS_RCP4.5	15.8	15.8	1	1.6	1.6	1	20.3	20.3	1	23.1	23.1	1
	ENS_RCP8.5	17.1	17.1	1	-0.8	-0.8	1	16.6	16.6	1	16.8	16.8	1
P2	CCCma_RCP4.5	13.9	13.9	1	-2.1	-2.1	1	-27.7	-27.7	1	-31.3	-31.3	1
	CCCma_RCP8.5	16.6	16.6	1	-4	-4	1	-28.4	-28.4	1	-34	-34	1
	HIRHAM5_RCP4.5	38.2	38.2	1	64.3	64.3	1	42.1	42.1	1	109	109	1
	HIRHAM5_RCP8.5	38.5	38.5	1	55.9	55.9	1	34.9	34.9	1	93	93	1
	RCA4_RCP4.5	14.4	14.4	1	12.1	12.1	1	21.9	21.9	1	35.3	35.3	1
	RCA4_RCP8.5	16.4	16.4	1	17.2	17.2	1	24.4	24.4	1	43	43	1
	REMO_RCP4.5	13.3	13.3	1	-3.5	-3.5	1	-12.6	-12.6	1	-16.9	-16.9	1
	REMO_RCP8.5	14.5	14.5	1	-4.3	-4.3	1	-13.2	-13.2	1	-18.3	-18.3	1
	ENS_RCP4.5	19.4	19.4	1	-0.4	-0.4	1	16.9	16.9	1	17.6	17.6	1
	ENS_RCP8.5	21	21	1	-1.5	-1.5	1	15.5	15.5	1	15	15	1
Bamendjing													
P1	CCCma_RCP4.5	6.7	6.7	1	14.4	14.4	1	-18.2	-18.2	1	-10.4	-10.4	1
	CCCma_RCP8.5	7.2	7.2	1	-5.7	-5.7	1	-7.6	-7.6	1	-15.9	-15.9	1
	HIRHAM5_RCP4.5	30.9	30.9	1	15.6	15.6	1	16	16	1	39	39	1
	HIRHAM5_RCP8.5	31.9	31.9	1	14.1	14.1	1	13.5	13.5	1	34.2	34.2	1
	RCA4_RCP4.5	6.7	6.7	1	12.6	12.6	1	12.9	12.9	1	30.2	30.2	1
	RCA4_RCP8.5	7.8	7.8	1	11.3	11.3	1	9.8	9.8	1	24.7	24.7	1
	REMO_RCP4.5	6	6	1	-3	-3	1	-10.3	-10.3	1	-17.2	-17.2	1
	REMO_RCP8.5	6.9	6.9	1	-2.5	-2.5	1	-12.3	-12.3	1	-19.3	-19.3	1
	ENS_RCP4.5	12.3	12.3	1	-4.8	-4.8	1	7.6	7.6	1	6.1	6.1	1
	ENS_RCP8.5	13.2	13.2	1	-6.9	-6.9	1	6.5	6.5	1	2.6	2.6	1
P2	CCCma_RCP4.5	3	3	1	15.4	15.4	1	-20	-20	1	-12.1	-12.1	1
	CCCma_RCP8.5	4.5	4.5	1	-7.7	-7.7	1	-9.8	-9.8	1	-21.1	-21.1	1
	HIRHAM5_RCP4.5	27.7	27.7	1	14.8	14.8	1	11.5	11.5	1	32.1	32.1	1
	HIRHAM5_RCP8.5	28.5	28.5	1	12.9	12.9	1	12	12	1	30.9	30.9	1
	RCA4_RCP4.5	3	3	1	12.5	12.5	1	12.6	12.6	1	29.7	29.7	1
	RCA4_RCP8.5	5.4	5.4	1	17.7	17.7	1	14.5	14.5	1	37.6	37.6	1
	REMO_RCP4.5	2.9	2.9	1	-3.4	-3.4	1	-13.7	-13.7	1	-22.3	-22.3	1
	REMO_RCP8.5	3.6	3.6	1	-2.1	-2.1	1	-9.9	-9.9	1	-15.7	-15.7	1
	ENS_RCP4.5	8.9	8.9	1	-4.9	-4.9	1	4.9	4.9	1	2.3	2.3	1
	ENS_RCP8.5	10.2	10.2	1	-6	-6	1	7.6	7.6	1	4.9	4.9	1

Table 7

Impact score of LULCC and CV on water balance components for the different periods, models and scenarios.

Periods	Models	PET		SURQ		GW_RCH		WYLD		
		Score LULCC	Score CV	Score LULCC	Score CV	Score LULCC	Score CV	Score LULCC	Score CV	
Mbakaou										
P1	CCCma_RCP4.5	1	0.08	1	0.08	1	0.08	1	0.08	
	CCCma_RCP8.5	1	0.08	1	0.08	1	0.08	1	0.08	
	HIRHAM5_RCP4.5	1	0.03	1	0.03	1	0.03	1	0.03	
	HIRHAM5_RCP8.5	1	0.03	1	0.03	1	0.03	1	0.03	
	RCA4_RCP4.5	1	0.08	1	0.08	1	0.08	1	0.08	
	RCA4_RCP8.5	1	0.08	1	0.08	1	0.08	1	0.08	
	REMO_RCP4.5	1	0.1	1	0.1	1	0.1	1	0.1	
	REMO_RCP8.5	1	0.08	1	0.08	1	0.08	1	0.08	
	ENS_RCP4.5	1	0.06	1	0.06	1	0.06	1	0.06	
	ENS_RCP8.5	1	0.05	1	0.05	1	0.05	1	0.05	
	P2	CCCma_RCP4.5	1	0.07	1	0.07	1	0.07	1	0.07
		CCCma_RCP8.5	1	0.06	1	0.06	1	0.06	1	0.06
		HIRHAM5_RCP4.5	1	0.02	1	0.02	1	0.02	1	0.02
		HIRHAM5_RCP8.5	1	0.07	1	0.07	1	0.07	1	0.07
RCA4_RCP4.5		1	0.07	1	0.07	1	0.07	1	0.07	
RCA4_RCP8.5		1	0.06	1	0.06	1	0.06	1	0.06	
REMO_RCP4.5		1	0.07	1	0.07	1	0.07	1	0.07	
REMO_RCP8.5		1	0.07	1	0.07	1	0.07	1	0.07	
ENS_RCP4.5		1	0.05	1	0.05	1	0.05	1	0.05	
ENS_RCP8.5		1	0.04	1	0.04	1	0.04	1	0.04	
Bamendjing										
P1	CCCma_RCP4.5	1	0.14	1	0.14	1	0.14	1	0.14	
	CCCma_RCP8.5	1	0.13	1	0.13	1	0.13	1	0.13	
	HIRHAM5_RCP4.5	1	0.03	1	0.03	1	0.03	1	0.03	
	HIRHAM5_RCP8.5	1	0.03	1	0.03	1	0.03	1	0.03	
	RCA4_RCP4.5	1	0.14	1	0.14	1	0.14	1	0.14	
	RCA4_RCP8.5	1	0.13	1	0.13	1	0.13	1	0.13	
	REMO_RCP4.5	1	0.16	1	0.16	1	0.16	1	0.16	
	REMO_RCP8.5	1	0.14	1	0.14	1	0.14	1	0.14	
	ENS_RCP4.5	1	0.08	1	0.08	1	0.08	1	0.08	
	ENS_RCP8.5	1	0.07	1	0.07	1	0.07	1	0.07	
	P2	CCCma_RCP4.5	1	0.33	1	0.33	1	0.33	1	0.33
		CCCma_RCP8.5	1	0.22	1	0.22	1	0.22	1	0.22
		HIRHAM5_RCP4.5	1	0.03	1	0.03	1	0.03	1	0.03
		HIRHAM5_RCP8.5	1	0.03	1	0.03	1	0.03	1	0.03
RCA4_RCP4.5		1	0.33	1	0.33	1	0.33	1	0.33	
RCA4_RCP8.5		1	0.18	1	0.18	1	0.18	1	0.18	
REMO_RCP4.5		1	0.34	1	0.34	1	0.34	1	0.34	
REMO_RCP8.5		1	0.27	1	0.27	1	0.27	1	0.27	
ENS_RCP4.5		1	0.11	1	0.11	1	0.11	1	0.11	
ENS_RCP8.5		1	0.09	1	0.09	1	0.09	1	0.09	

6.5. Forecast reliability

To find out which RCM is the most reliable, the corrected historical data from the various models for the period 2001–2005 (historical) have been integrated into the SWAT hydrological model, to simulate the flows over this interval, knowing that the observed flows are available over this period. A comparison was then made between observed flows and simulated flows from historical RCMs data, the idea being that the most reliable RCM forecasts are those of the RCM for which the data from the historical period allow us to better simulate the observed flows.

Fig. 11 shows that the curve of average monthly flows observed is closer to that of the flows simulated from the data of the REMO model and the average of all the models. This is confirmed by a study of the statistical relationship between the compared datasets (Fig. 12 and Table 8). The observed and simulated flows from the REMO model data show the best statistical relationship in the case of the Mbakaou basin, with a respective R^2 and NSE of 0.86 and 0.85. With a respective R^2 and NSE of 0.83 and 0.8, the relationship between observed and simulated flows based on the average of the models ranks second. For the Bamendjing basin, these same datasets display the best statistical relationships with an R^2 and NSE greater than 0.75 (Fig. 12).

Individually, the REMO model is the one for which historical data appears to be closest to observed data. The trend and deviations it predicts for precipitation and runoff also appear to be the most consistent, based on historical trends highlighted from observed data. The quality of a forecast is also assessed by taking into account the consistency it shows with historical trends. The REMO model predicts a drop in precipitation that does not reach -19% regardless of the basin, the period and the scenario considered. This trend seems consistent insofar as the region is experiencing a drop in rainfall that started in the 1970 s (Mahé et al., 1990; Sighomnou, 2004; Ebodé, 2022). So far, no study has contradicted this trend or demonstrated a sudden reversal of the latter in recent decades. It therefore seems more logical to think that this decline will continue as shown by the REMO model, rather than to believe in a sudden reversal

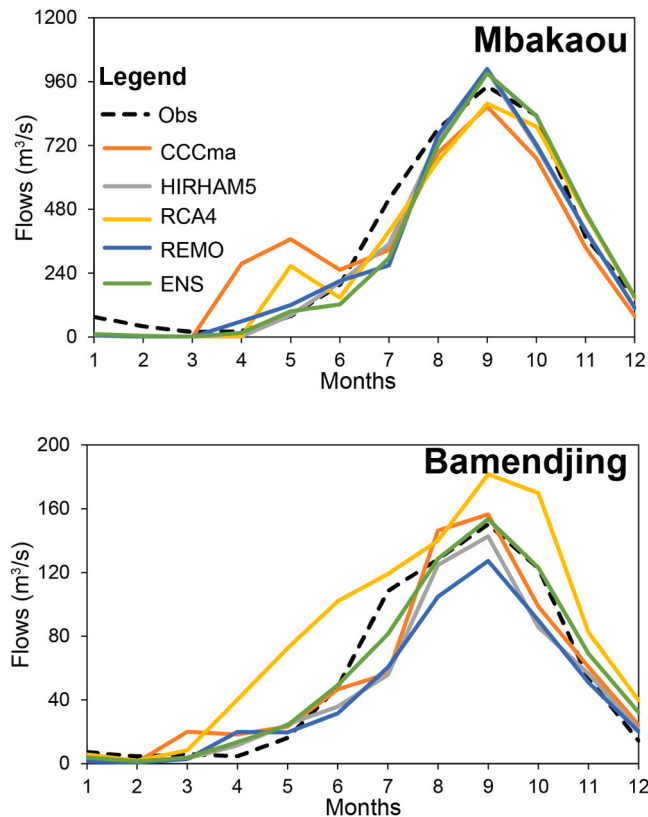


Fig. 11. Comparison between observed and simulated flows (from meteorological model data) during the historical period (2002–2005) at monthly time scale.

from the year 2024 as predicted by the HIRHAM5 and RCA4 models.

7. Conclusion

This study aimed to assess the availability of the current water resource and its future evolution in two regulated sub-basins of the Sanaga River, but also to separate the respective impact of LULCCs and CV on the variability of this resource. For this, the SWAT (Soil and Water Assessment Tool) hydrological model, certain meteorological and spatial reference data available for the region (Merra2, Landsat, etc.) and outcomes of regional climate models (RCMs) (RCA4, CCCma, HIRHAM5 and REMO) were used. It appears that in these basins, the groundwater recharge (GW_RCH), flows, water yield (WYLD) and sediment load (SED) are more important in the middle zone. Conversely, runoff (SURQ) is low in this part of the basins. Potential evapotranspiration (PET), for its part, seems to be greater to the east of the basins. Two models (REMO and CCCma) predict a decrease in precipitation, water balance components (WBCs) and SURQ. Two others (HIRHAM5 and RCA4) provide the opposite (increase). The REMO model is the one for which the forecasts seem to be the most reliable. A statistical study carried out over the historical period (2001–2005) demonstrated that the flows simulated from the data of this model are closer to the observed flows. This statistical relationship materializes in the case of Mbakaou by an R^2 and NSE greater than 0.8. In the case of Bamendjing, the calculated R^2 and NSE are above 0.75. Concerning land use and land cover (LULC), it is expected that their future changes will be very low, given that the investigated basins have almost no forest left (land cover pattern which undergoes the most human pressure in the region). These small changes will have no impact on flows. Climate variability (CV) is the only forcing whose impact will be perceptible in future flows. The impact scores of these forcings on the WBCs prove this sufficiently. The impact scores of CV are equal to 1. However, those of LULC are all less than 0.09. Ultimately, it appears that alternative data (satellite data, model data, etc.) are a relevant solution to the data problem which hampers modelling work in certain regions like the one investigated. However, this study certainly achieved good results, but these results could have been significantly better if they were based on observed data. Permanent monitoring of the region's basins is therefore necessary.

Funding

This research received no external funding.

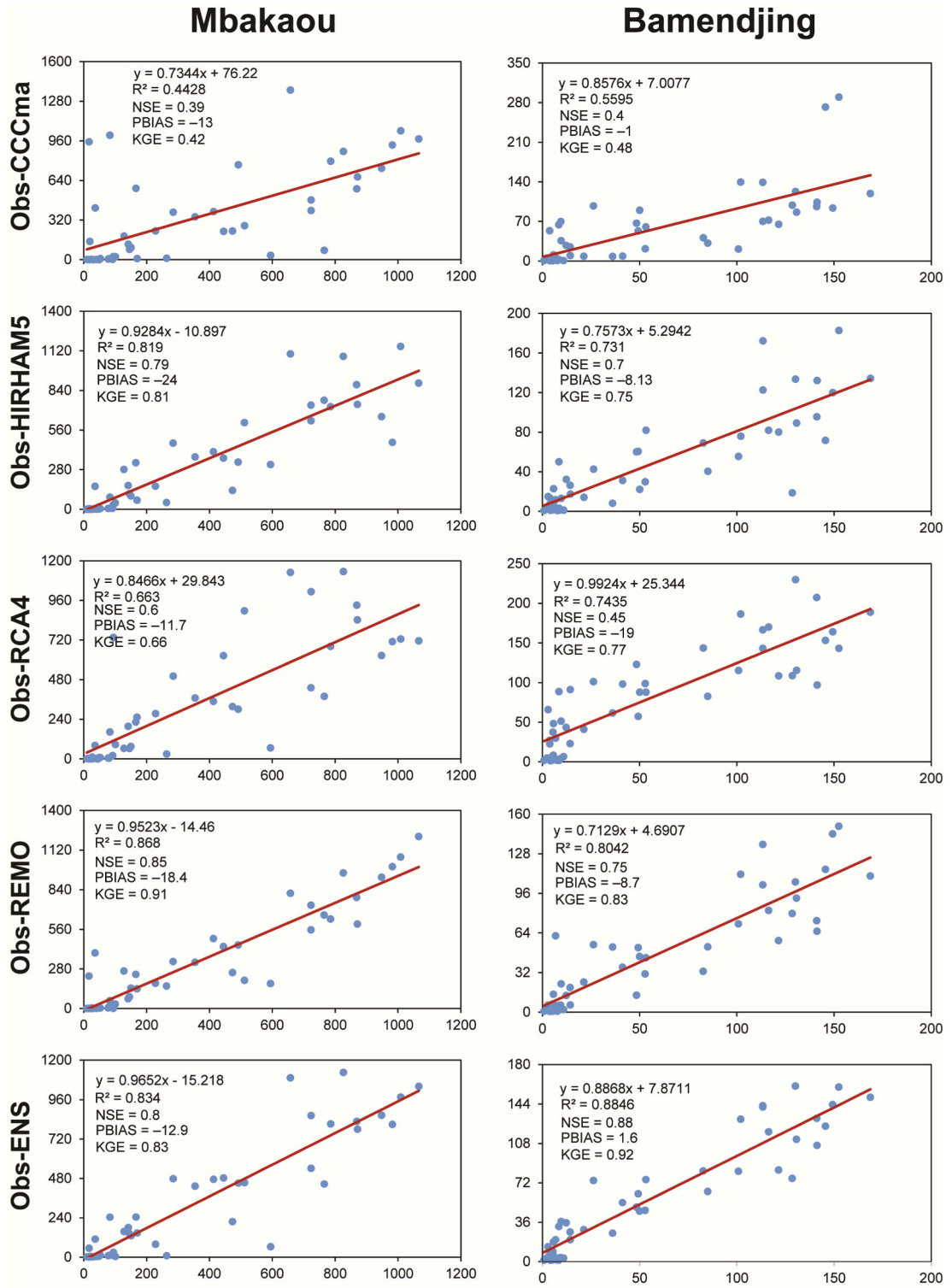


Fig. 12. Relationship between observed and simulated flows (from meteorological model data) during the historical period (2002–2005) at monthly time scale.

Table 8

Basic statistics related to monthly observed and simulated discharges during the historical period (2002–2005).

Statistics	Observed	CCCma	HIRHAM5	RCA4	REMO	ENS
Mbakaou						
Mean (m ³ /s)	356	301	282	317	296	301
Standard deviation	44	98	83	101	59	78
Coefficient of variation	0.12	0.33	0.29	0.32	0.20	0.26
Bamendjing						
Mean (m ³ /s)	55	53	41	38	40	57
Standard deviation	7	18	11	12	6	8
Coefficient of variation	0.13	0.34	0.27	0.32	0.15	0.14

CRedit authorship contribution statement

Jean Riotte: Writing – review & editing, Writing – original draft, Validation. **Bérenger Koffi:** Writing – original draft, Software, Methodology. **Gil Mahé:** Validation, Supervision, Project administration. **Jean Jacques Braun:** Validation, Supervision. **Jean Guy Dzana:** Methodology, Formal analysis, Data curation, Conceptualization. **Valentin Brice Brice Ebodé:** Software, Methodology, Investigation, Funding acquisition, Formal analysis, Data curation, Conceptualization. **Sakaros Bogning Dongué:** Writing – original draft, Software, Investigation, Formal analysis. **Raphael Onguéné:** Writing – review & editing, Writing – original draft, Funding acquisition, Formal analysis, Data curation, Conceptualization.

Declaration of Competing Interest

The authors declare there is no conflict.

Data availability

Data will be made available on request.

References

- Abbott, M.B., Bathurst, J.C., Cunge, J.A., O'connell, P.E., Rasmussen, J., 1986. An introduction to the European Hydrological System—Système Hydrologique Européen SHE 2, Structure of a physically based distributed modelling system. *J. Hydrol.* 87, 61–77. [https://doi.org/10.1016/0022-1694\(86\)90114-9](https://doi.org/10.1016/0022-1694(86)90114-9).
- Akoko, G., Le, T.H., Gomi, T., Kato, T.A., 2021. Review of SWAT model application in Africa. *Water* 13, 1313. <https://doi.org/10.3390/w13091313>.
- Ardoin-Bardin, S., Dezetter, A., Servat, E., Paturel, J.E., Mahé, G., Niel, H., Dieulin, C., 2009. Using general circulation model outputs to assess impacts of climate change on runoff for large hydrological catchments in West Africa. *Hydrol. Sci. J.* 54 (1), 77–89.
- Arnold, J.G., Srinivasan, R., Muttiah, R.S., Williams, J.R., 1998. Large area hydrologic modeling and assessment part I. Model Dev. *J. Am. Water Resour. Assoc.* 34, 73–89. <https://doi.org/10.1111/j.1752-1688.1998.tb05961.x>.
- Arnold, J.G., Kiniry, J.R., Srinivasan, R., Williams, J.R., Haney, E.B., Neitsch, S.L., 2012. Soil and water assessment tool: input/output documentation. Version 2012, TR-439, Texas Water Resources Institute, College Station, USA.
- Awotwi, A., Annor, T., Anornu, G.K., Quay-Ballard, J.A., Agyekum, J., Ampadu, B., Nti, I.K., Gyampo, M.A., Boakye, E., 2021. Climate change impact on streamflow in a tropical basin of Ghana, West Africa. *J. Hydrol.: Reg. Stud.* 34, 100805 <https://doi.org/10.1016/j.ejrh.2021.100805>.
- Basheer, A., Lü, H., Omer, A., Ali, A., Abdelgader, A., 2015. Impacts of Climate Change under CMIP5 RCP Scenarios on the Streamflow in the Dinder River and Ecosystem Habitats in Dinder National Park, Sudan. *Hydrol. Earth Syst. Sci. Discuss.* 12, 10157–10195. <https://doi.org/10.5194/hessd-12-10157-2015>.
- Bennour, A., Jia, L., Menenti, M., Zheng, C., Zeng, Y., Barnieh, B., Jiang, M., 2023. Assessing impacts of climate variability and land use/land cover change on the water balance components in the Sahel using Earth observations and hydrological modelling. *J. Hydrol.: Reg. Stud.* 47, 101370.
- Beven, K.J., Kirkby, M.J., 1979. A physically based, variable contributing area model of basin hydrology. *Hydrol. Sci. Bull.* 24, 43–69. <https://doi.org/10.1080/02626667909491834>.
- Bejene, T., Lettenmaier, D.P., Kabat, P., 2010. Hydrologic impacts of climate change on the Nile River Basin: implications of the 2007 IPCC scenarios. *Clim. Change* 100, 433–461. <https://doi.org/10.1007/s10584-009-9693-0>.
- Bigot, S., Philippon, N., Gond, V., Moron, V., Pokam, W., Bayol, N., Boyemba, F., Kahindo, B., Samba, G., Ngomanda, A., Gapia, M., Yongo, O.D., Laurent, J.-P., Gourlet-Fleury, S., Doumengé, C., Forni, E., Camberlin, P., Martiny, N., Dubreuil, V. & Brou, T. 2016 Etat actuel des réseaux de mesure éco-climatiques en Afrique centrale: Les ambitions du projet de recherche internationale FORGREENE. XXIXe Colloque de l'Association Internationale de Climatologie, Lausanne - Besançon, Suisse.
- Bodian, A., Dezetter, A., Dacosta, A., 2012. Apport de la modélisation pluie-débit pour la connaissance de la ressource en eau: application au haut Bassin du Fleuve Sénégal. *Climatologie* 9, 109–125. <https://doi.org/10.4267/climatologie.223>.
- Chang, H.J., Jung, I.W., 2010. Spatial and temporal changes in runoff caused by climate change in a complex large river basin in Oregon. *J. Hydrol.* 388 (3), 186–207. <https://doi.org/10.1016/j.jhydrol.2010.04.040>.
- Chen, H., Xu, C.-Y., Guo, S., 2012. Comparison and evaluation of multiple GCMs, statistical downscaling and hydrological models in the study of climate change impacts on runoff. *J. Hydrol.* 434, 36–45. <https://doi.org/10.1016/j.jhydrol.2012.02.040>.
- Dibaba, W.T., Miegel, K., Demissie, T.A., 2019. Evaluation of the CORDEX Regional climate models performance in simulating climate conditions of two catchments in Upper Blue Nile Basin. *Dyn. Atmospheres Oceans* 87, 101104. <https://doi.org/10.1016/j.dynatmoce.2019.101104>.
- Dibaba, W.T., Demissie, T.A., Miegel, K., 2020. Watershed Hydrological Response to Combined Land Use/Land Cover and Climate Change in Highland Ethiopia: Finchaa Catchment. *Water* 12, 1801. <https://doi.org/10.3390/w12061801>.
- Dosdogru, F., Kalin, L., Wang, R., Yen, H., 2020. Potential impacts of land use/cover and climate changes on ecologically relevant flows. *J. Hydrol.* 584, 124654 <https://doi.org/10.1016/j.jhydrol.2020.124654>.
- Ebodé, V.B., 2022. Impact of rainfall variability and land-use changes on river discharge in Sanaga catchment (forest–savannah transition zone in Central Africa). *Hydrol. Res.* 53 (7) <https://doi.org/10.2166/nh.2022.046>.
- Ebodé, V.B., Mahé, G., Dzana, J.G., Amougou, J.A., 2020. Anthropization and Climate Change: Impact on the Discharges of Forest Watersheds in Central Africa. *Water* 12, 2718. <https://doi.org/10.3390/w12102718>.

- Ebodé, V.B., Dzana, J.G., Nkiaka, E., Nka, N.B., Braun, J.J., Riotte, J., 2022. Effects of climate and anthropogenic changes on current and future variability in flows in the So'o River Basin (south of Cameroon). *Hydrol. Res.* 53 (9), 1203–1220. <https://doi.org/10.2166/nh.2022.047>.
- Elaji, A., Ji, W., 2020. Urban Runoff Simulation: How Do Land Use/Cover Change Patterning and Geospatial Data Quality Impact Model Outcome? *Water* 2020 12, 2715. <https://doi.org/10.3390/w12102715>.
- Faramarzi, M., Abblaspour, K.C., Schulin, R., Yang, H., 2009. Modelling blue and green water resources availability in Iran. *Hydrol. Process.* 23, 486–501. DOI: [10.1002/hyp.7160](https://doi.org/10.1002/hyp.7160).
- Gadissa, T., Nyadawa, M., Behulu, F., Mutua, B., 2018. The effect of climate change on loss of lake volume: case of sedimentation in Central Rift Valley Basin, Ethiopia. *Hydrology* 5 (4), 67. <https://doi.org/10.3390/hydrology5040067>.
- Hadour, A., Meddi, M., Mahe, G., 2020. Watershed Based Hydrological Evolution Under Climate Change Effect: An Example From North Western Algeria. *Journal Of Hydrology, Regional Studies* 28, <https://doi.org/10.1016/J.Ejrh.2020.100671>.
- Halmly, M.W.A., Gessler, P.E., Hicke, J.A., Salem, B.B., 2015. Land use/land cover change detection and prediction in the north-western coastal desert of Egypt using Markov-CA. *Appl. Geogr.* 63, 101–112. <https://doi.org/10.1016/j.apgeog.2015.06.015>.
- Hyandye, C.B., Worqul, A., Martz, L.W., Musuka, A., 2018. The impact of future climate and land use/cover change on water resources in the Ndembera watershed and their mitigation and adaptation strategies. *Environ Syst Res.* 7, 7. <https://doi.org/10.1186/s40068-018-0110-4>.
- Kingston, D.G., Taylor, R.G., 2010. Sources of uncertainty in climate change impacts on river discharge and groundwater in a headwater catchment of the Upper Nile Basin, Uganda. *Hydrol. Earth Syst. Sci.* 14, 1297–1308. <https://doi.org/10.5194/hess-14-1297-2010>.
- Knutti, R., Furrer, R., Tebaldi, C., Cernak, J., Meehl, G.A., 2010. Challenges in Combining Projections from Multiple Climate Models. *J. Clim.* 23 (10), 2739–2758.
- Koffi, B., Brou, A.L., Kouadio, K., Ebodé, V.B., N'guessan, K., Yangouliba, Y., Yaya, K., Brou, D., Kouassi, K., 2023. Impact of climate and land use/land cover change on Lobo reservoir inflow, West-Central of Côte d'Ivoire. *J. Hydrol.: Reg. Stud.* 47, 101417. <https://doi.org/10.1016/j.ejrh.2023.101417>.
- Lambin, E.F., Geist, H.J., Lepers, E., 2003. Dynamics of land-use and land-cover change in tropical regions. *Annu. Rev. Environ. Resour.* 28, 205–241. <https://doi.org/10.1146/annurev.energy.28.050302.105459>.
- Mahé, G., Lericque, J., Olivry, J.C., 1990. L'Ogooué au Gabon. Reconstitution des débits manquants et mise en évidence de variations climatiques à l'équateur. *Hydrol. Cont.* 5, 105–124.
- Mendez, M., Calvo-Valverde, L., 2016. Development of the HBV-TEC Hydrological Model. *Procedia Eng.* 154, 1116–1123. <https://doi.org/10.1016/j.proeng.2016.07.521>.
- Moriassi, D.J., Arnold, J.G., Van Liew, M.W., Bingner, R.L., Harmel, R.D., Veith, T.L., 2007. Model evaluation guidelines for systematic quantification of accuracy in watershed simulations. *Am. Soc. Agric. Biol. Eng.* 50, 885–900.
- Mwangi, J., Shisanaya, C., Gathanya, J., Namirembe, S., Moriassi, D., 2015. A Modeling Approach to Evaluate the Impact of Conservation Practices on Water and Sediment Yield in Sasumua Watershed, Kenya. *J. Soil Water Conserv.* 70, 75–90. <https://doi.org/10.2489/jswc.70.2.75>.
- Neitsch, S.L., Arnold, J.G., Kiniry, J.R., Williams, J.R., 2005. Soil and water assessment tool: theoretical documentation. USDA, Agricultural Research Service, Blackland Research Center, Texas A&M University, USA, 494 p.
- Rathjens, H., Bieger, K., Srinivasan, R., Chaubey, I., Arnold, J.G., 2016. CMhyd User Manual. Available online: <http://swat.tamu.edu/software/cmhyd/> (accessed on 4 January 2021).
- Reshmidevi, T., Kumar, D.N., Mehrotra, R., Sharma, A., 2018. Estimation of the climate change impact on a catchment water balance using an ensemble of GCMs. *J. Hydrol.* 556, 1192–1204.
- Ruelland, D., Ardoin-Bardin, S., Collet, L., Roucou, P., 2012. Simulating future trends in hydrological regime of a large Sudano-Sahelian catchment under climate change. *J. Hydrol.* 424–425 (6 207–216). <https://doi.org/10.1016/j.jhydrol.2012.01.002>.
- Setegn, S.G., Srinivasan, R., Melesse, A.M., Dargahi, B., 2010. SWAT Model Application and Prediction Uncertainty Analysis in the Lake Tana Basin, Ethiopia. *Hydrol. Process.* 24, 357–367. <https://doi.org/10.1002/hyp.7457>.
- Sighomnou, D., 2004. Analyse et redéfinition des régimes climatiques et hydrologiques du Cameroun: perspectives d'évolution des ressources en eau. Thèse de Doctorat d'Etat, Université de Yaounde I, 290 p.
- Taleb, R.B., Naimi, M., Chikhaoui, M., Raclot, D., Sabir, M., 2019. Evaluation Des Performances Du Modèle Agrohydrologique SWAT à Reproduire Le Fonctionnement Hydrologique Du Bassin Versant Nakhla (Rif occidental, Maroc). *Eur. Sci. J.* 15, 311–333. <https://doi.org/10.19044/esj.2019.v15n5p311>.
- Tegegne, G., Park, D.K., Kim, Y.O., 2017. Comparison of hydrological models for the assessment of water resources in a data-scarce region, the Upper Blue Nile River Basin. *J. Hydrol. Reg. Stud.* 14, 49–66. <https://doi.org/10.1016/j.ejrh.2017.10.002>.
- Teutschbein, C., Seibert, J., 2012. Bias correction of regional climate model simulations for hydrological climate-change impact studies: Review and evaluation of different methods. *J. Hydrol.* 456–457, 12–29. <https://doi.org/10.1016/j.jhydrol.2012.05.052>.
- Wang, S., Zhang, Z., Sun, G., Strauss, P., Guo, J., Tang, Y., Yao, A., 2012. Multi-site calibration validation, and sensitivity analysis of the MIKE SHE Model for a large watershed in northern China. *Hydrol. Earth Syst. Sci.* 16, 4621–4632. <https://doi.org/10.5194/hess-16-4621-2012>.
- Yang, C., Wu, G., Chen, J., Li, Q., Ding, K., Wang, G., Zhang, C., 2019. Simulating and forecasting spatio-temporal characteristic of land-use/cover change with numerical model and remote sensing: a case study in Fuxian Lake Basin, China. *Eur. J. Remote Sens.* 52 (1), 374–384. <https://doi.org/10.1080/22797254.2019.1611387>.
- Yin, Z., Feng, Q., Yang, L., Wen, X., Si, J., Zou, S., 2017. Long-term quantification of climate and land cover change impacts on streamflow in an alpine river catchment, northwestern China. *Sustain* 9. <https://doi.org/10.3390/su9071278>.
- Yira, Y., Diekkrüger, D., Steup, D., Bossa, Y.A., 2017. Impact of climate change on hydrological conditions in a tropical West African catchment using an ensemble of climate simulations. *Hydrol. Earth Syst. Sci.* 21, 2143–2161. <https://doi.org/10.5194/hess-21-2143-2017>.
- Zhang, B., Shrestha, N.K., Daggupati, P., Rudra, R., Shukla, R., Kaur, B., Hou, J., 2018. Quantifying the Impacts of Climate Change on Streamflow Dynamics of Two Major Rivers of the Northern Lake Erie Basin in Canada. *Sustainability* 10 (8), 2897. <https://doi.org/10.3390/su10082897>.
- Zhang, H., Huang, G.H., 2013. Development of climate change projections for small watersheds using multi-model ensemble simulation and stochastic weather generation. *Clim. Dyn.* 40 (3–4), 805–821. <https://doi.org/10.1016/j.jhydrol.2014.06.037>.
- Zhang, H., Wang, B., Liu, D.L., Zhang, M., Fenga, P., Cheng, L., Yu, Q., Eamus, D., 2019. Impacts of future climate change on water resource availability of eastern Australia: A case study of the Manning River basin. *J. Hydrol.* 573, 49–59. <https://doi.org/10.1016/j.jhydrol.2019.03.067>.
- Zhang, Y., Tang, C., Ye, A., Zheng, T., Nie, X., Tu, A., Zhu, H., Zhang, H., 2020. Impacts of Climate and Land-Use Change on Blue and Green Water: A Case Study of the Upper Ganjiang River Basin, China. *Water* 12, 2661. <https://doi.org/10.3390/w12102661>.
- Zhao, Z., Wang, H., Bai, Q., Wu, Y., Wang, C., 2020. Quantitative analysis of the effects of natural and human factors on a hydrological system in Zhangweinan Canal Basin. *Water* 12, 1864. <https://doi.org/10.3390/w12071864>.